by residents; 2)Learning based modules for techniques and diagnostic procedures; 3)Resources from basic concepts to advanced topics; 4)Board review material and questions in interactive formats.
Results: Multiple learning modules incorporating reference material, web based resources and teleconferences, and procedures were constructed in a format that would be intuitive for most residents to use. Distinct sections for basic terminology, lab management, and board review materials were included. Additionally 3 video presentations (10-12 min long) were provided to residents as part of a didactic lecture series. In an anonymous survey residents (7/14) evaluated the portal as excellent and plan to use it to gain molecular competency and for board reviews. The videos were rated as good to excellent.
Conclusions: With ever expanding medical knowledge in this molecular era, the portal based training modules will be a central part of a comprehensive resident training in molecular pathology. The current "one size fits all" approach would be altered to best fit the residents' interests in different molecular subspecialty after completion of basic training in molecular pathology. This web based portal will help system based training for residents in smaller programs where these state of the art molecular assays are not offered. This type of portal will make all these supplementary educational materials available to pathologists, medical students, and laboratory technologists which may also serve as proficiency testing.

578 Using Digital Bone and Soft Tissue Tumor Pathology Teaching Library To Enhance Training of Future Pathologists

X Zhang, JJ Johnson, MC Lloyd, D Letson, MM Bui. University of South Florida College of Medicine, Tampa, FL; H. Lee Moffitt Cancer Center, Tampa, FL.
Background: The training of residents in bone and soft tissue tumor pathology has been limited in most of the training programs due to the rarity of the tumor, difficulty in diagnosis, and lack of expertise. Whole slide digital imaging technology has increasing role in the education of pathologist trainees. We envision that a virtual bone and soft tissue tumor pathology teaching library will greatly enhance training. This study is to investigate the feasibility and effectiveness of this alternative paradigm for education and assessment.
Design: The project was done collaboratively by pathology residents, sarcoma pathologist, sarcoma surgeon, radiologist, and scientists at digital imaging lab. Representative glass slides were retrospectively selected using the WHO Bone and Soft Tissue Tumor Classification (2006). De-identified slides were scanned using AperioScanScope XT. The effectiveness between traditional method using glass slides and the alternative method using digital slides in sarcoma learning was evaluated.
Results: As one of the premier cancer centers and sarcoma programs, we are able to collect 2,000 cases of bone and soft tissue tumors listed in the WHO book which include 120 types. Currently 351 bone and soft tissue virtual slides are in the library. High-resolution digital images of whole slides can be viewed at any work station using a password protected server. The virtual images were organized and annotated to incorporate diagnosis, clinical information and key pathologic findings. A web browser based interface with search engine features is being constructed. The library can be accessed from the work stations outside Moffitt when residents are rotating in other hospitals or at home. Residents using the alternative leaning method scored higher than the residents using the traditional method.
Conclusions: A digital bone and soft tissue tumor pathology teaching library is feasible for both a sarcoma center and non-sarcoma centers via internet, thus beyond the limitation of resources. It is an effective tool in educating residents in bone and soft tissue pathology. It is one time investment which will last indefinitely. For the future, the library will be expanded to educate related specialties including orthopedic surgeons and musculoskeletal radiologists.

Endocrine

579 Cytoplasmic Staining of OCT4 in Pheochromocytoma Is Highly Sensitive and Specific: A Novel Immunohistochemical Finding

RE Alexander, DJ Grignon, MT Idrees. Indiana University School of Medicine, Indianapolis, IN.
Background: OCT4 immunostaining has become an essential resource in the diagnosis of germ cell neoplasia. OCT4 is a transcription factor and has a characteristic nuclear staining specific to germ cell neoplasms. The diagnosis of adrenal malignancy is sometimes challenging and it is often difficult to establish a diagnosis on morphology alone, especially in metastatic cases. In our institute, it has been observed that paraganglionic tissue consistently displayed intense cytoplasmic staining and we intended to determine if OCT4 can provide additional diagnostic utility in adrenal tumors. To our knowledge, the cytoplasmic expression of OCT4 in pheochromocytoma has not been specifically studied. The goal of this study is to analyze the immunoreactivity of adrenal cortical carcinoma (ACC) and pheochromocytoma, especially in metastatic settings.
Design: Thirty cases of primary pheochromocytoma, 24 cases of ACC (two metastatic), and 8 cases of metastatic pheochromocytoma were selected from our database. Hematoxylin and eosin (H&E) stained slides were reviewed and OCT4 (MRQ-10, Mouse monoclonal, Cell Marque Corp.; Rocklin CA, ready to use) immunostaining was performed. OCT4 staining was scored on a four-tier system (0-3), judging two separate criteria: intensity and extent of staining.
Results: In 30 of 30 (100%) cases of primary pheochromocytoma, strong and diffuse (3+3) immunoexpression was observed. In metastatic pheochromocytoma, all cases showed diffuse staining. Six of 8 (75%) metastatic pheochromocytomas showed strong expression (3+3), the remaining two (25%) showed moderate intensity (2+3). In 24 of 24 (100%) cases of ACC, including metastatic cases, OCT4 was completely negative. In all positive staining pheochromocytoma cases, the staining pattern was uniformly cytoplasmic. Nuclei were overshadowed by cytoplasmic staining in most cases. Controls, using seminoma, stained in an appropriate nuclear fashion.
Conclusions: The results describe a novel staining pattern for OCT4 in pheochromocytoma. This staining pattern has not been demonstrated elsewhere and appears to be highly specific and sensitive to paraganglionic tissue. These findings suggest that OCT4 is an immunostain with diagnostic implications in adrenal neoplasms. The difference in staining pattern may be reactivity to an unknown cross-reacting cytoplasmic antigen and needs further analysis. Additional immunoelectron microscopic and comparative studies using different commercially available OCT4 antibodies may be helpful in determining the cytoplasmic antigen.

580 Papillary Thyroid Carcinoma with Hobnail Features: Histopathological Criteria To Predict Aggressive Behavior

S Asioli, LA Erickson, A Righi, RV Lloyd. Department of Biomedical Sciences and Human Oncology, University of Turin, Turin, Italy; Department of Laboratory Medicine and Pathology, Mayo Clinic, Rochester, MN; University of Wisconsin School of Medicine and Public Health, Madison, WI.
Background: Recent reports indicate that papillary thyroid carcinoma (PTC) with hobnail features (micropapillary variant of papillary thyroid carcinoma, MPTC) is a rare, but very aggressive variant of PTC. We examined 23 cases of MPTC to determine the prognostic significance of the amount of micropapillary or hobnail features in these tumors.
Design: The histopathological and immunohistochemical features of 23 MPTC were examined. Follow up information was obtained from medical record review. The patients included 17 females and 6 males. Ages ranged from 28 to 78 (mean 57). Tumor size ranged from 1 to 5.8 cm (mean 3 cm). The average follow-up time was 106 months (range: 4 to 272 months).
Results: Twelve cases (52.2%) of MPTC showed more than 30% micropapillary or hobnail features and all but 3 cases were associated with an aggressive behavior during follow-up. In particular, all but two cases showed lymph node metastases at presentation. During follow-up, 6 of these patients died of disease after a mean of 44.8 months and 3 patients remained alive with extensive disease involving the epiglottis, larynx, and nasopharynx in two cases and the shoulder, lung, bone, muscle, and pancreas in one case after a mean follow-up of 32.3 months. The other 3 patients with prominent micropapillary or hobnail features were alive without evidence of disease after a mean follow-up of 125.3 months.The other 11 PTC cases (47.8%) showed less than 30% micropapillary or hobnail features. Eight of these patients were alive without disease after a mean of 169 months and one patient died of sepsis which was not related to thyroid tumor after 155 months. Two patients in this group died of disease after 21 and 163 months respectively.
Conclusions: These findings confirm earlier observations that MPTC is an aggressive variant of PTC. Tumors with more than 30% hobnail features were often very aggressive, although two patients with tumors with less than 10% hobnail features also had poor outcomes.

581 Beta-HCG Producing Anaplastic Thyroid Carcinoma – A Variant with Improved Prognosis?

N Becker, RD Chernock, B Nussenbaum, JS Lewis. Washington University School of Medicine, St. Louis, MO.
Background: Anaplastic thyroid carcinoma (ATC) is a rare malignancy which is clinically very aggressive. The median survival is 5 months after diagnosis. No treatment is associated with a significant improvement in survival. Recently, we identified what we believe is the first case of a beta-hCG secreting ATC. It responded dramatically to chemotherapy and radiation and was subsequently surgically resected. The patient's serum beta-hCG was 53 IU/L at diagnosis and dropped to 6 IU/L two weeks after surgery. After 14 months, the patient has no evidence of disease or detectable serum beta-hCG. Although beta-hCG secretion has been reported in many neoplasms, it has not yet been described in ATC.
Design: After characterization of the sentinel beta-hCG secreting case, which was strongly positive in almost all tumor cells for beta-hCG and negative for PAX8, an additional 29 cases of anaplastic thyroid carcinoma were retrieved from our files and immunostained for beta-hCG and PAX8. Staining was graded for intensity (weak, moderate, strong) and distribution (quartiles) by 3 study pathologists. Clinical follow up information was obtained by chart review.
Results: Beta-hCG staining was present in five of 30 cases (17%), but only the sentinel case showed strong, diffuse staining. The remaining positive cases showed either strong beta-hCG staining in <25% of cells, or moderate staining in up to 75% of the cells. PAX8 staining was present in 18 of 30 (60%) cases, including two of the five (40%) beta-hCG positive cases. Follow up of the beta-hCG positive patients showed that only the index case was treated with chemoradiation and surgery. The remaining beta-hCG positive patients either went to hospice or received palliative treatment only. Twenty-seven of 29 patients died of disease at a median of 3.3 months, including all four additional beta-hCG positive patients at a median of 2.7 months. PAX8 positive cases had improved overall survival (median survival 4.9 months versus 2.0 months; p=0.0164).
Conclusions: Our study demonstrates the first beta-hCG secreting ATC. It was treatment responsive and has had a provisionally favorable outcome. Four additional cases showed beta-hCG expression but none was treated with curative intent. Although only a single case, our findings suggest that strongly beta-hCG positive ATC may be a unique entity within the larger group. In addition, our results suggest that PAX8 expression by ATC may correlate with a better prognosis.

582 Clinico-Pathological and Molecular Characteristics of Tall Cell Variant of Papillary Thyroid Microcarcinoma

J Bernstein, R Virk, WH Westra, G Tallini, P Hui, R Udelsman, CT Sasaki, S Roman, JA Sosa, ML Prasad. Yale School of Medicine, New Haven, CT; Johns Hopkins School of Medicine, Baltimore, MD; Bologna University School of Medicine, Bologna, Italy.

Background: Papillary thyroid microcarcinomas (PTMC) are papillary thyroid carcinomas (PTC) measuring ≤1 cm. Their prognosis is excellent. However, a subset of them behave aggressively with recurrence, metastasis and cancer-specific mortality of up to 2%. The tall cell variant of PTC is a particularly aggressive tumor that generally presents in advanced stage and is associated with higher disease-related mortality. Recognizing this variant in PTMC may help select aggressive microcarcinomas for a more intensive therapy.

Design: Clinico-pathological features of 12 tall cell variant (TCV) PTMC in 10 patients were reviewed. DNA was extracted from tumor tissue and *BRAF* V600E mutational analysis was performed by single stranded conformational polymorphism electrophoresis.

Results: The patients included 8 women and 2 men aged 34 to 66 years (mean 52.8 years). All patients underwent total thyroidectomy. Nine of ten thyroids (90%) contained multifocal PTMC. In 2 thyroids both tumors were TCV while in the remaining 7 thyroids the additional PTMCs were classic types. Nine TCV were located within the left lobes and three in the right lobes. The tumors varied from 3 mm to 10 mm in size (mean 6.5 mm). The tumor cells had moderate to abundant eosinophilic cytoplasm and the majority of them were at least twice as tall as wide. The nuclear features were those of classic PTC and intranuclear inclusions were frequent. All tumors were associated with fibrosis and a minimal lymphocytic response (100%). All but one of the tumors exhibited an infiltrative interface with the non-neoplastic thyroid (92%). None of the tumors were cystic or exhibited psammoma bodies. Three tumors exhibited extrathyroidal extension (pT3) and three showed lymphovascular invasion (25%). Lymph nodes were dissected in seven patients, and showed metastases (43%) to level VI nodes in one (pN1a) and lateral cervical lymph nodes in 2 patients (pN1b). Nine of eleven tumors had *BRAF* V600E mutations (82%). Two TCV with wild-type BRAF arose within the same thyroid, both were subcapsular and one showed extrathyroidal extension and lymphovascular invasion.

Conclusions: The tall cell variant of papillary microcarcinoma is frequently associated with multifocality, extrathyroidal extension, advanced nodal stage at presentation and *BRAF* V600E mutation. Recognition of TCV among the papillary microcarcinomas may help select patients for more aggressive treatment.

583 Thyroid Rests or Malignancy: Can BRAF Mutation Analysis Help in the Differential Diagnosis?

A Best, C Chisholm, D Smith, MK Lopez, K Walker, RS Beissner, A Rao. Scott & White Memorial Hospital and Texas A&M Health Science Center College of Medicine, Temple, TX.

Background: Thyroid rests can pose diagnostic challenges for status of metastatic disease in papillary thyroid carcinoma (PTC). BRAF V600E mutations are commonly seen in PTC and may indicate aggressive behavior. Mutational status can serve to differentiate metastases from benign rests. To our knowledge, only one case has reported in which a benign-appearing thyroid rest in a cervical lymph node was reclassified as a PTC metastasis by testing for the BRAF V600E mutation. We present the first case series in which BRAF mutation status is investigated in multiple lymph nodes with thyroid rests.

Design: We identified 20 cases of thyroid rests from 1988-2011. 13 were diagnosed as benign and seven were indeterminate as benign versus metastatic. 10/13 benign rests were in patients with PTC; five had other metastases. 3/13 cases were discovered incidentally, not in the context of a known PTC. All seven indeterminate rests were in cases of PTC; four had metastases in other nodes. Five control cases of metastatic PTC in lymph nodes and five primary PTC's without metastases were identified. Cells from areas of interest were laser-captured, amplified using Quiagen's BRAF Pyro Kit and analyzed on the PryoMark Q24 sequencer.

Results: BRAF mutations were not identified in the 20 benign and indeterminate rests, including cases with metastases to lymph nodes. Five of the 10 benign-appearing rests had metastases in other nodes: two had BRAF mutation in the primary and in the metastasis, and three had the mutation in the primary but not in the metastasis. In the other five cases, three had BRAF mutation in the primary and two did not. 4/7 indeterminate cases had metastases in other nodes: two had BRAF mutations in the primary and in the metastases, one had the mutation in the primary only, and one had the mutation in the metastasis only. 3/7 were without metastases and had BRAF mutations in the primary. 4/5 PTC control cases with metastases had the BRAF mutation in the primary only, and one was negative. 4/5 PTC control cases without metastases had BRAF mutation and one did not.

Table 1. Statistical data

Sensitivity	Specificity	PPV	NPV
66%	100%	100%	53%

Conclusions: BRAF mutations in nodes has a high PPV, with mutations only identified in metastatic foci. The NPV is lower because PTC metastases may alter mutational status. Importantly, the benign-appearing and indeterminate rests were all were negative for BRAF mutations. BRAF status is an effective means to differentiate benign thyroid rests from PTC metastases.

584 Proposal for a Simplified Mib1 Assessment in Pancreatic Endocrine Tumors

A Blank, L Boos, I Zlobec, P Komminoth, A Perren, AM Schmitt. University of Bern, Bern, Switzerland; Technical University Munich, Munich, Germany; City Hospital Triemli, Zurich, Switzerland.

Background: The prediction of biological behavior in pancreatic endocrine tumors (PET) is challenging in the absence of metastases. The WHO 2010 classification requires grading by assessment of the Mib1 index. This requires counting of 2000 cells in a hot-spot. As this procedure is not easily performed in clinical routine the aim of the present study was to test a simplified assessment of the proliferation index in PET.

Design: In a first step Mib1 staining was examined by counting the number of positive tumor cells per HPF (0.2mm^2) in TMA punches of 133 primary sporadic PET. In a second step using whole slide sections of the same cohort Mib1 positive tumor cells were counted in 1mm^2 in the centre and in the periphery of the tumor.

ROC analysis was performed to obtain the optimal cut-off for the number of tumor cells positive for Mib1 regarding risk stratification. Results were correlated with Mib1 proliferation index (2%) as well as with survival data.

Results: Overall the number of Mib1 positive tumor cells correlated significantly with the Mib1 proliferation index. ROC analysis showed a cut-off of ≤7 tumor cells/0.2mm^2 staining with Mib1 for an optimal risk stratification on the TMA in the present cohort. On whole slide sections, in the center of the tumor the mean value of positive tumor cells was the best predictor for disease-free survival, whereas in the periphery of the tumor the maximum value of positive tumor cells was the best predictor for disease-free survivial. No such difference could be detected regarding disease-specific survival.

Conclusions: In the present study we demonstrate a simplified method to assess the proliferation of PET by counting the number of tumor cells staining with Mib1. This method could substitute for the presently recommended proliferation index.

585 Follicular Variant of Papillary Thyroid Carcinoma (FVPTC): Histological Features, BRAF Mutation, and Lymph Node Metastasis

S Bose, SK Mohanty, C Singh, A Riley-Portuges, W Sacks, AE Walts. Cedars-Sinai Medical Center, Los Angeles, CA; University of Minnesota, Minneapolis, MN.

Background: FVPTC is currently treated the same as conventional papillary thyroid carcinoma (PTC). Recent reports indicate that well circumscribed FVPTC has a low BRAF mutation rate (similar to follicular neoplasms) whereas infiltrative FVPTC has a higher BRAF mutation rate (similar to conventional PTC) raising the possibility that histopathology and/or BRAF mutation status might help stratify FVPTC. This study aims to correlate histological features and BRAF mutation status in FVPTC with lymph node metastases.

Design: Slides of 56 FVPTC [20 with metastases to regional lymph node(s) (LNP) and 36 with negative regional lymph node(s) (LNN)] were retrieved from our files and reviewed. Patient demographics and tumor focality, size, circumscription, follicular architectural distortion, solid foci, intratumoral fibrosis, encapsulation (capsular integrity, thickness), capsular and lymphvascular invasion (LVI), extrathyroidal extension (ETE), and margin status were charted. Macrodissected formalin fixed paraffin embedded sections from 43 (20 LNP and 23 LNN) of the FVPTC were analyzed for BRAF V600E (1799T>A) mutation using real-time PCR. Correlations between the categorical variables were assessed by Fisher's exact, chi-square, and/or t-test(s) with two-sided $p<0.05$ considered significant.

Results: The patients (46 female, 10 male) ranged from 24 to 75 years in age (median 51 yrs). BRAF mutation was detected in 5(25%) LNP and in 7(30%) LNN FVPTC. Comparison of the LNP and the LNN groups revealed significant differences in pT-stage, tumor focality, and in the extent of circumscription, follicular architectural distortion, solid foci, papillae, LVI, and ETE. No significant difference was observed in age, gender, tumor size, intratumoral fibrosis, completeness of capsule, capsular thickness, capsular invasion, or margin status. Although BRAF mutation was detected more frequently in unencapsulated FVPTC and in cases with LVI, no significant difference was noted in the prevalence of BRAF mutation between the LNP and LNN groups.

Conclusions: -Tumor focality, circumscription, follicular architectural distortion, solid foci, papillae, LVI, ETE and pT-stage are each significant predictors of nodal involvement by FVPTC.

-In FVPTC, BRAF mutation status does not appear to correlate with lymph node metastasis.

586 Expression of Epithelial-Mesenchymal Transition Regulators Slug and Twist in Thyroid Carcinomas

D Buehler, H Hardin, W Shan, W Rehrauer, H Chen, RV Lloyd. University of Wisconsin School of Medicine and Public Health, Madison, WI.

Background: Epithelial-mesenchymal transition (EMT) has been recognized as an important mechanism of epithelial tumor progression, local invasion and metastasis. The E-cadherin repressor Slug and the basic helix-loop-helix transcription factor Twist inhibit E-cadherin expression in poorly differentiated malignancies as inducers of EMT. Very little is known about the expression of EMT regulators in thyroid cancer. In this study, we examined the expression of Twist, Slug and E-cadherin in a panel of well-differentiated and anaplastic thyroid carcinomas by immunohistochemistry and by RT-PCR in thyroid cell lines.

Design: 10 anaplastic thyroid carcinomas (ATC), 28 follicular carcinomas, 56 papillary thyroid carcinomas (PTC) including 28 follicular variants, 33 follicular adenomas and 10 normal thyroids (NT) were assembled on a tissue microarray using triplicate 0.6 mm cores and examined for expression of E-cadherin, Slug and Twist by immunohistochemistry. Unequivocal nuclear staining for Slug and Twist and membranous staining for E-cadherin were considered for interpretation. Immunoreactivity was scored based on the percentage of cells stained and the intensity

of staining. Focal or diffuse moderate or strong staining was considered to be positive. The expression of E-cadherin, Slug and Twist mRNA was tested in various thyroid cell lines including 2 NT, two PTC and 3 ATC.
Results: Most (8/10) ATCs showed strong nuclear immunoreactivity for Slug (6 cases diffuse, 2 cases focal). In five cases (62.5%), Slug expression was associated with absence of E-cadherin. None of the NTs, follicular adenomas, and follicular or papillary carcinomas were immunoreactive for Slug ($p<0.0001$). All cases of NTs, adenomas and well-differentiated thyroid carcinomas were positive for E-cadherin. Twist was expressed in 5/10 ATCs, but not in NTs, adenomas or well-differentiated carcinomas ($p<0.001$). By RT-PCR, E-cadherin was expressed in the NT and PTC cell lines only, while Slug and Twist were expressed in both the PTC and ATC cell lines.
Conclusions: The EMT regulators Slug and Twist are expressed in anaplastic thyroid carcinomas and are associated with absence of E-cadherin supporting the role of EMT in this cancer. E-cadherin expression was present in all normal thyroids, follicular adenomas and well-differentiated carcinomas and none of these lesions expressed Slug or Twist. Expression of the EMT marker mRNAs was more complex in cell lines. Immunohistochemical detection of Slug and Twist may be helpful in diagnostically challenging cases of thyroid tumors in limited biopsy samples.

587 Cell Cycle Regulators in Pheochromocytomas (PCTs) and Paragangliomas (PGLs) and Correlation with SDHx Status and FGFR4 Genotype

CA Cassol, SL Asa. University Health Network, Toronto, ON, Canada.
Background: Proliferation and apoptosis evasion are hallmarks of cancer. Cell cycle (CC) regulators (cyclins and CDKs) promote CC progression through Rb inactivation, while CC inhibitors such as p16, p21, p27, p53 and p57 prevent it. In this study, we investigated the expression of CC regulators and inhibitors in PCTs/PGLs and correlated the results with SDHB IHC and FGFR4 G388R genotype.
Design: PCTs (N=39) and PGLs (N=76) from 115 patients of known FGFR4-G388R genotype were assembled in a TMA stained with antibodies against p16, p21, p27 KIP1, p53, Ki67, Cyclin D1, Rb and SDHB. TMA slides were scanned and analyzed using Spectrum Plus (Aperio). Immunostaining scores and outcomes were used for exploratory statistical analysis on SPSS 11.0.
Results: In 115 patients, there were 13 outcomes - 4 local recurrences, 7 metastases and 2 deaths - all from PGLs. SDHB IHC showed loss in 46 cases, of which only one was a PCT. All but one metastasis occurred in SDHB IHC-negative cases. The CC inhibitors p16 ($p=0.002$), p27 ($p=0.001$), p21 ($p=0.044$) and Rb ($p=0.007$) were overexpressed in PGLs compared to normal adrenal medulla. Conversely, they were underexpressed in PCTs, with exception of p16, which was also overexpressed ($p<0.001$). The percentage of p53 positive nuclei was very low in both PCTs (3%),PGLs (1.2%), and normal adrenal medullas (2.5%). MIB1 was overexpressed in PGLs (4%) when compared to PCTs (0.8%, $p<.0001$) and normal medulla (1.3%, $p=0.004$); it was also associated with an increased risk for metastasis ($p=0.008$). The percentage of cells with cytoplasmic staining for p27 was higher in metastatic cases (53.5% versus 39%, $p=0.045$), as was MIB1 nuclear staining (5.8% versus 2.5%, $p=0.002$). The percentage of Cyclin D1 nuclear staining was higher in FGFR4 Gly^{388} cases (70%) than in FGFR4 Arg^{388} (60%), $p=0.002$; while the percentage of p53 nuclear staining was lower ($p=0.014$). Comparison between SDHB-positive and -negative tumors showed significant underexpression of p16 in SDHB negative cases ($p=0.014$) and overexpression of Cyclin D1 ($p=0.004$) and MIB1 (4.3% versus 1.7%, $p<0.001$).
Conclusions: The different patterns of expression of cell cycle inhibitors between PGLs and PCTs reflect their different biology and behavior and warrant further investigation. The low percentage of p53 staining is in accordance with previous studies showing a very low frequency of p53 mutations in these tumors. SDHB-negative and FGFR4 Gly^{388} cases seem to have higher proliferative activity. A high MIB1 index was significantly associated with malignancy, as well as with SDHB loss.

588 Effect of Subspecialty Sign-Out on the Diagnosis of Follicular-Patterned Thyroid Neoplasms

DJ Chute, TM Elsheikh, AP Hoschar. Cleveland Clinic, Cleveland, OH.
Background: The diagnosis of follicular variant of papillary thyroid carcinoma (FVPTC) can be quite challenging when nuclear features are subtle or borderline. Several studies have demonstrated significant interobserver and intraobserver variation in the diagnosis of FVPTC, even among expert head and neck pathologists. On July 1st, 2003 our institution switched from a general pathology sign-out to subspecialty sign-out system. In this study, we examine trends in the diagnosis of follicular patterned thyroid neoplasms, including FVPTC, before and after this change.
Design: Primary thyroid resections containing follicular-patterned neoplasms were identified over a period of 16 years (8 years prior to and 8 years after the change in sign-out systems). Only neoplasms with pure follicular growth pattern were examined, including: follicular adenoma (FA), Hürthle cell adenoma (HCA), follicular carcinoma (FC), Hürthle cell carcinoma (HCC), and follicular variant of papillary thyroid carcinoma (FVPTC). Cases of papillary microcarcinoma were excluded from the study. The number of primary thyroid resections with each neoplasm type was tabulated along with the total number of thyroid resections over each time period.
Results: In the first 8 years of the study (pre subspecialty sign-out), there were 1,866 thyroid resections, out of which 258 (13.8%) follicular patterned neoplasms were retrieved. These included133 FA (52%), 37 HCA (14%), 30 FC (11%), 13 HCC (5%), and 46 FVPTC (18%). In the latter 8 years of the study (post subspecialty sign-out) there were 3,535 thyroid resections, out of which 324 (9%) follicular patterned neoplasms were retrieved. These included 108 FA (33%), 34 HCA (10%), 28 FC (9%), 19 HCC (6%), and 138 FVPTC (42%). There was an apparent rapid rise and a statistically significant increase in reporting FVPTC ($p<0.001$) in association with the onset of subspecialty sign-out. The decrease in reporting FA was statistically significant ($p<0.001$), but had a slow decline with acceleration in recent years. There was no significant difference in reporting of HCA, FC, or HCC.
Conclusions: Subspecialty sign-out with expert head and neck pathologists was associated with a significant increase in the diagnosis of FVPTC, and a decline in reporting FAs. This may be due to better recognition by head and neck subspecialty pathologists or better overall awareness of subtle papillary carcinoma nuclear features over time.

589 microRNA Expression Array Identifies Novel Diagnostic Markers for Conventional and Oncocytic Follicular Thyroid Carcinomas

M Dettmer, MB Durso, P Komminoth, H Moch, A Perren, YE Nikiforov, MN Nikiforova. University of Pittsburgh, Pittsburgh; Triemlispital, Zurich, Switzerland; University Hospital, Zurich, Switzerland; University of Bern, Bern, Switzerland.
Background: Follicular carcinoma (FTC) and oncocytic follicular carcinoma (oFTC) represent thyroid tumors that frequently pose diagnostic challenge, both on cytologic and histopathologic analysis. Several miRNAs have been previously reported as reliable markers in conventional papillary thyroid carcinomas, however, limited information is available for FTC and oFTC. The aim of this study was to identify candidate miRNA markers that can be used diagnostically.
Design: Forty two follicular thyroid carcinomas (21 FTC, 21 oFTC) and 11 normal thyroid tissues were studied for expression of 380 miRNAs using Human Microarray Assays (Applied Biosystems) on ABI7900. miRNAs were isolated using Trizol reagents from frozen thyroid tissue (n=18) and using RecoverAll Total Nucleic Acid kit (Ambion) from FFPE tissue specimens (n=24). Data analysis was performed with Data Assist v3.0 (Applied Biosystems) program. Expression of candidate miRNA markers was individually validated in all samples by RT-PCR.
Results: Both types of folicular carcinomas (FTC and oFTC) demonstrated deregulatation in miRNA expression as compared to normal thyroid tissue with significant number of downregulated miRNAs and several upregulated miRNAs. Overall, the levels of miRNA expression were different between these tumor groups and the unsupevised hierarchical clustering analysis revealed individual cluster for oFTC and FTC. miRNAs upregulated in both tumor types were miR-182 (3-8 folds), miR-183 (4-7 folds), miR-221 (3-30 folds), and miR-222 (2-10 folds) and miRNAs strongly (>4 folds) downregulated were 199a-3p and miR-455-5p. Moreover, extremely high upregulation of miR-885-5p (34-56 folds, $p<0.01$) was detected only in oFTC.
Conclusions: This study shows different miRNA expression profiles in FTC and oFTC, supporting a notion that they represent independent tumor subtypes. Several miRNAs were found sugnificantly upregulated and downregulated in follicular carcinomas as compared to normal thyroid. miR-885-5p is a novel miRNA found to be highly upregulated in oFTCs and can be used as a diagnostic marker of oFTC in surgical and FNA samples.

590 Tall Cell Variant of Papillary thyroid Carcinoma – How Many Tall Cells Are Needed?

MS Dettmer, A Schmitt, H Steinert, H Moch, P Komminoth, A Perren. University of Pittsburgh, Pittsburgh, PA; University of Bern, Bern, Switzerland; University Hospital Zurich, Zurich, Switzerland; Triemlispital, Zurich, Zurich, Switzerland.
Background: Differentiated papillary thyroid cancers (PTC) have a favorable 5-year survival rate of >95%. However, it is difficult to identify patients with an adverse clinical outcome (ACO). The tall cell variant of PTC (TCV) is known to have an ACO, but there are different diagnostic criteria in the literature.
Design: We evaluated histomorphologic criteria in 126 patients with PTC. To enhance the portion of papillary carcinomas with an ACO, we collaborated with all nuclear medicine departments of the Canton, Zürich. 56 patients with an ACO, defined as more than one relapse or tumor related death were identified. They were compared with a control group (CG) of 70 age-stage-gender-matched PTC. All tumors were reevaluated by three pathologists. The tumor type was determined according to the 2004 WHO classification and the percentage of tall cells (TC) in the PTCs was measured semiquantitatively. TCs were defined to be more than three times as high as wide.
Results: We found 48 TCV (38%), with a cut off of 10% TC per PTC, and 78 PTCs without any TC (62%). Kaplan-Meier analysis demonstrated a significantly worse overall survival (OS), tumor specific survival (TSS) and relapse free survival (RFS) ($P<0.001$) in patients with tumors containing an area composed of 10% or more TCs. TC above 10% was the only constant significant factor in a multivariate analysis (COX regression) for the OS, TSS and RFS, including age, stage and gender.
Conclusions: A 10% TC-quantity within a papillary carcinoma is strongly associated with an ACO and should therefore be reported. Following studies must show whether patients with such tumors benefit from additional therapy.

591 EGFR Expression and V600E BRAF Mutations Influence Disease Progression in Thyroid Carcinoma

KE Fisher, CE Hill, C Foulks, CJ Weber, J Sharma, C Cohen. Emory University, Atlanta, GA.
Background: The worldwide incidence of thyroid carcinoma is steadily rising with a concomitant increase in disease-associated mortality. Activating mutations in *BRAF* are associated with aggressive disease in papillary thyroid carcinoma (PTC). Epidermal growth factor receptor (EGFR) is an upstream receptor in the BRAF signaling pathway and is overexpressed in anaplastic carcinoma (APC). We investigated how oncogenic mutations in *BRAF* and *EGFR* and EGFR protein expression influenced disease outcomes in the four major thyroid carcinoma subtypes: PTC, follicular (FC), medullary (MC), and APC.

Design: Two pathologists scored 79 cases of thyroid carcinoma from a TMA for EGFR intensity (0–3+) and percent positivity (0–100%). High EGFR expression (EGFR-H) was defined as 3+ staining or 2+ staining of ≥ 50% of cells. DNA was successfully extracted from single paraffin blocks of 59 cases for mutational analysis (MA). Activating *BRAF* V600E (T→A 1799) or *EGFR* exon 21 L858R (T→G 2573) mutations, or *EGFR* exon 19 deletions (del 2235-2249/2236-2250; del E746-A750) were determined using pyrosequencing. The subtypes tested (IHC/MA) included PTC (23/18), FC (35/33), MC (9/2), APC (12/6), and unclassifiable (1/1). Statistical significance was determined using Fisher's exact test.

Results: In PTC, EGFR-H correlated with lymph node (LN) metastases ($p< 0.01$) but not with survival or recurrence. EGFR expression increased the risk of recurrence in Hurthle cell variant of FC ($p= 0.054$). EGFR-H was seen in all APCs (12/12). No EGFR expression was seen in MC (0/9). None (0/59) of the carcinomas demonstrated *EGFR* exon 19 deletions or exon 21 activating mutations. 10% (6/59) of the carcinomas harbored V600E *BRAF* mutations (2 APCs and 4 metastatic PTCs) and all 6 expressed high levels of EGFR by IHC. V600E *BRAF* mutations correlated with LN metastases ($p< 0.01$) and 50% (3/6) of patients with BRAF mutations survived <6 months.

Conclusions: EGFR expression increased the risk of recurrence in Hurthle cell variant of FC, and EGFR-H correlated with LN metastases in PTC. V600E *BRAF* mutations were associated with LN metastases and decreased survival. No E746-A750 deletions or L858R *EGFR* mutations were identified by pyrosequencing suggesting that alternate mechanisms for EGFR overexpression are involved in thyroid carcinogenesis. The finding that all cases of V600E *BRAF* mutations coexpressed EGFR-H suggests that in thyroid carcinomas unlike in lung adenocarcinomas, EGFR expression and downstream BRAF activating mutations may not be mutually exclusive.

592 Less Tumor Distance to Thyroid Pseudo Capsule Is Associated with Local Recurrence and Distant Metastases of Microscopic Papillary Carcinoma

A Gamboa-Dominguez, B Camacho-Dominguez, M Chapa-Ibarguengoitia, V Rosas-Camargo, O Gonzalez-Trevino. Instituto Nacional de Ciencias Medicas y Nutricion SZ, Mexico City, DF, Mexico.

Background: Studies of microscopic carcinoma (mPC) of the thyroid frequently does not separate persistence vs recurrent disease. A search for prognostic factors and the influence of tumor distance to thyroid pseudocapsule in mPC was our aim.

Design: A retrospective review of all thyroid specimens since 1968 through mid 2008 was performed searching for mPC. The number of tumors, size, location and its distance to thyroid pseudocapsule was measured. Ultrasonographic studies were re-evaluated and a blind search of suspicious lesions was performed. Demographic, clinical, surgical, and ^{131}I administration were obtained from charts. TSH, T3, T4 and the clinical features were correlated with sonographic or tomographic data. Persistent disease was diagnosed when uninterrupted high TSH levels were identified after surgery or when metastases were evident during the first six months of follow-up, afterwards were considered as recurrences.

Results: A total of 1,343 thyroid specimens were evaluated and 511 PTC were identified in 40 years. 59(4.39%) were identified with mPC. Male to female ratio was 1:14 affecting mainly young patients (median age 43 years), with multiple tumors(51%) and bilateral affection(30%). Median tumor size was 7mm and cervical metastases observed in 42%. None with distant metastasis. Total or subtotal thyroidectomies were achieved in 50 persons, 36% with lymph node dissection. All but four patients received ^{131}I. Tumor contact with thyroid pseudocapsule was documented in 13 patients. Ultrasonographic location of suspicious nodule was possible in 12. After 10y follow-up(17-480 months), 55 patients had uneventful follow-up, three had local lymph node recurrences and one mediastinal and lung metastases. These four received ^{131}I and had tumors in contact with pseudocapsule. Nine patients with tumors in contact with pseudocapsule were free of metastases.

Association of tumor location to thyroidal pseudocapsule. Initial presentation and outcome after surgical and medical treatment of microscopic papillary carcinoma

	0mm	1-3mm	>4mm	TOTAL
Uneventful follow-up	9	34	12	55
Local recurrence	3	0	0	3
Distant metastases	1	0	0	1
TOTAL	13	34	12	59

A 3X3 contingency table showed chi2 with four grades of freedom p=0.004

Adverse factors were mPC contact with pseudocapsule*(p=0.0016)* and extra thyroid disease at the beginning*(p=0.02)*. No influence was observed for age, gender, focality, bilaterality, size, +ve nodes or type of surgery.

Conclusions: Close location to pseudocapsule of ≤10mm papillary thyroid carcinoma is an adverse finding.

593 Prognostic Implications of Papillary Thyroid Carcinoma with Tall Cell Features

I Ganly, T Ibrahimpasic, M Rivera, I Nixon, F Palmer, SG Patel, A Shaha, RM Tuttle, JP Shah, R Ghossein. Memorial Sloan-Kettering Cancer Center, New York, NY.

Background: The impact of the diagnosis of a papillary thyroid carcinoma (PTC) with tall cell features (TCF) on survival is unknown.

Design: All PTC patients identified at a single institution between 1985 and 2005 were analyzed. Classical PTC (cPTC) were defined as having <30% tall cells, PTC TCF (30-49% tall cells), tall cell variant (TCV) (≥50% tall cells). All cPTC, PTC TCF and TCV ≥ 1 cm in size were included.

Results: 453 patients satisfied the inclusion criteria (288 cPTC, 31 PTC TCF and 134 TCV). cPTC patients were much younger than their PTC TCF and TCV counterparts ($p<0.0002$). There was an increase in tumor size from cPTC to PTC TCF and TCV ($p=0.05$). Extensive extra-thyroid extension was more often present in TCV and PTC TCF (55%, 52% respectively) than in cPTC (33%) ($p=0.0001$). Margins were more frequently positive in TCV and PTC TCF (16%,17% respectively) than in cPTC (9%) ($p=0.03$). Overall pathologic tumor (pT) stage was more advanced in TCV and TCV TCF (19%, 22% pT 4 respectively) than in cPTC (7% pT4) ($p<0.0001$). Total thyroidectomy was more often performed on TCV patients (87%) than on their PTC TCF (68%) and cPTC (70%) counterparts ($p=0.014$). Radioactive iodine therapy was more frequently administered to TCV (74%) than to PTC TCF (58%) and cPTC (52%) patients ($p=0.0001$). Median follow up was 9.3 years. 10 year disease specific survival (DSS) was lower in TCV (96%) and PTC TCF (91%) than in cPTC (100%) ($p<0.001$). 10 year distant recurrence free (RFS) survival was higher in cPTC (98%) than in PTC TCF (89%) and TCV (96%) ($p=0.03$). Within the group of patients with extensive extra-thyroid extension, TCV and PTC TCF had a poorer DSS and distant RFS than cPTC($p=0.006$, $p=0.04$ respectively). Multivariate analysis could not be performed for DSS since only 6 patients died of disease.

Conclusions: 1) PTC TCF and TCV have the same clinico-pathologic features (e.g older age, advanced stage) that are more aggressive than cPTC 2) PTC TCF and TCV have similar DSS and distant RFS survival but poorer than classical PTC 3) PTC TCF are currently being treated like cPTC less aggressively than TCV 4) Consideration should be given to use a 30% tall cells threshold to diagnose TCV.

594 Large Adrenal Cortical Adenomas with Extensive Myelolipomatous Metaplasia: Upregulation of Jak-Stat Pathway and Solitary Fibrous Type Stromal Reaction

E Garratt, A Blanes, SJ Diaz-Cano. Barts and The London Hospitals, London, United Kingdom; University of Malaga School of Medicine, Malaga, Spain; King's College Hospital, London, United Kingdom.

Background: The presence of extensive myelolipomatous metaplasia (MLM) is rare in adrenocortical neoplasms, and the biological reasons are unknown. We investigate the cell survival and proliferation pathways and the stromal reaction in these neoplasms.

Design: We selected adrenocortical adenomas (ACA, 82; 8 with extensive/multifocal MLM), ACTH-independent nodular hyperplasias with no dominant nodules (ACNH, 23), and carcinomas (ACC, 22) (WHO criteria) to analyze cell survival-proliferation pathways (MKI67, ERK1, AKT1, CASP3, BCL2, CCND1, FN1, JUN, MMP7, MYC, BMP1, BMP7, TERT, IGF2), and stromal-inflammatory reaction types (CDH11, SDC1, SPARC, MMP11, CSF1, CD68, CD163, FCGR2, CXCL9, IL4, IL4R, IRF1, MMP10) in a low-density selective cDNA array. Total RNA was extracted, cleaned from normal and neoplastic tissues (RNeasy columns), first-strand cDNA synthesized using T7-(dT24)-oligomer and used as template for cRNA synthesis. The cRNA was fragmented, Cy3-/Cy5-labeled, and hybridized to arrays noncompetitively, cross-validating the results (expression factor>2, significance<0.01). Variables were studied regarding MLM presence and histological diagnosis. Significant variables were then tested on tissue sections by in-situ techniques.

Results: Multifocal and extensive MLM was only observed in ACA: ACA+MLM were significantly bigger (7.9±1.5cm, 142.6±9.9g) than the remaining ACA, and they showed bone metaplasia and positive PET scan in 7/8 cases. ACA with MLM showed significant upregulation (expression factor>2, $p<0.01$) for AKT1, BMP1, TERT, CCND1, CD68, CD163, and IL4/IL4R (when compared with ACC), and for CASP3, FN1, CXCL9, IL4, BMP1, CD68, MMP11 (when compared with ACNH and conventional ACA). Remaining genes showed no significant differences.

Conclusions: ACA with MLM is worth recognizing because it is frequently be confused preoperatively with ACC due to its bigger size and positive PET scan. Biologically, this pattern is related with the tumor upregulation of Jak-Stat pathway (CXCL9, IL4, IL4R), downregulation of PI3k/AKT pathway (AKT1, CCND1, CASP3) and solitary fibrous type stromal reaction (CD68, CD163) from BMP1 producing ACA.

595 ACTH-Independent Multinodular Adrenal Hyperplasia with Dominant Nodule: Expression Profile Support a Neoplastic-Like and Non-Functional Presentation

E Garratt, A Blanes, SJ Diaz-Cano. Barts and The London Hospitals, London, United Kingdom; University of Malaga School of Medicine, Malaga, Spain; King's College Hospital, London, United Kingdom.

Background: ACTH-independent multinodular adrenal hyperplasia is a heterogeneous disease, some of them presenting with dominant nodules that can be difficult to differentiate from adrenal adenomas. We investigate the contributions of Jak-Stat pathways and cell growth-proliferation pathways in this process.

Design: We selected ACTH-independent nodular hyperplasias with (12, AIMAH) and without (23, ACNH) dominant nodule (3:1 size ratio with second biggest), adrenocortical adenomas (ACA, 74), and carcinomas (ACC, 22) (WHO criteria) to analyze PI3 Kinase/AKT pathway (AKT1, BCL2, CCND1, FN1, JUN, MMP7, MYC), CREB pathway (CYP19A1, EGR1, FOS), Jak-Stat pathway (CXCL9, IL4, IL4R, IRF1, MMP10, NOS2A), and cell growth-proliferation (MKI67, TERT, CAV2, EGFR, ERBB3, FGFBP1, IGF2, IGFBP4, MST1R, PDGFRB, TGFB1, TGFB2, TGFB3) in a low-density selective cDNA array. Total RNA was extracted, cleaned from normal and neoplastic tissues (RNeasy columns), first-strand cDNA synthesized using T7-(dT24)-oligomer and used as template for cRNA synthesis. The cRNA was fragmented, Cy3-/Cy5-labeled, and hybridized to arrays noncompetitively, cross-validating the results (expression factor>2, significance<0.01). Variables were studied regarding histological diagnosis and presence of dominant nodule. Significant variables were then tested on tissue sections by in-situ techniques.

Results: AIMAH revealed significant downregulation of CCND1, FN1, CYP19A1, CXCL9, IL4, ERBB3, and MST1R; and upregulation of AKT1, JUN, CAV2, and TGFB2. All these markers segregated differently in the comparison AIMAH vs. ACC.

The differential markers with benign lesions were: TERT, CCND1, and TGFB2 with ACNH; JUN, and CYP19A1 with ACA. Remaining genes showed no significant differences.

Conclusions: AIMAH expression profile reveals a non-inflammatory (downregulation of key markers of Jak-Stat pathway), and antiapoptotic (AKT1 and TFGB2 pathways) background that contribute to longer cell survival (TERT upregulation) and neoplastic-like expansion. Down-regulaton of JUN and CYP19A1 would contribute to a lower cellular functionality and a clinical presentation with mass effect.

596 Endocrine Tumors Display Site-Specific Alterations in Wnt Signaling, the mTOR Pathway, and Chromatin Remodeling

PS Ginter, NC Panarelli, RK Yantiss, T Scognamiglio, Y-T Chen. Weill Cornell Medical College, New York.

Background: Endocrine tumors (ET) comprise a heterogeneous group of neoplasms that affect multiple organ systems, yet genetic alterations in these sporadic tumors are poorly defined. Some ET of the bronchi, gastrointestinal (GI) tract, and adrenal cortex show B-catenin mutations, whereas mTOR pathway activation and mutations in the chromatin remodeling genes, *ATRX* and *DAXX*, are thought to be crucial to pancreatic ET pathogenesis. In this study, we evaluated the expression of B-catenin, mTOR pathway proteins, ATRX and DAXX in ET from various organs to determine their potential roles in the pathogenesis of ET.

Design: Tissue microarrays were constructed from low-to-intermediate grade ET (Ki-67 index <20%), including 50 parathyroid adenomas, 50 adrenocortical adenomas, 46 pituitary adenomas, 51 bronchial carcinoid tumors, and 60 well-differentiated ET of the GI tract [27 small intestinal, 10 appendiceal, and 23 pancreatic]. TMAs were stained for B-catenin, p-mTOR, PTEN, TSC2, ATRX and DAXX. Aberrant staining was defined as nuclear staining for B-catenin, increased (2+ to 3+) cytoplasmic mTOR staining, decreased (0 to 1+) cytoplasmic staining for TSC2 and PTEN, and staining of <50% of nuclei for ATRX and DAXX.

Results:

Immunohistochemical Analysis of Endocrine Tumors (in percentages)

	Small Intestinal ET (n=27)	Appendiceal ET (n=10)	Pancreatic ET (n=23)	Bronchial Carcinoid (n=51)	Adrenocortical Adenoma (n=50)	Pituitary Adenoma (n=46)	Parathyroid adenoma (n=50)
Nuclear B-catenin	0	0	0	0	86	0	0
Increased mTOR	78	100	38	52	6	52	52
Decreased PTEN	89	50	74	24	98	28	96
Decreased TSC2	100	50	74	90	94	48	92
Decreased ATRX	77	50	57	51	88	4	14
Decreased DAXX	81	80	65	49	24	6	4

Nuclear B-catenin was only noted in adrenocortical adenoma (86%). Increased mTOR was most frequent in small intestinal and appendiceal ET (>75%), lower in others. PTEN and TSC2 showed parallel losses in ET of most organs except the bronchi. Loss of ATRX or DAXX was found in the majority of GI and bronchial ET, but not in pituitary or parathyroid adenoma.

Conclusions: Alterations in the mTOR pathway are globally present in ET of multiple organs, but aberrant Wnt-signaling is limited to adrenocortical adenomas. Small intestinal ET most frequently exhibit alterations in the mTOR pathway and chromosome remodeling proteins, which less commonly involve the foregut-derived bronchial and pancreatic ET. Loss of chromosome remodeling proteins was often seen in ET of the diffuse endocrine system (GI, pancreas, bronchi), but was much less common in ET from endocrine organs (adrenal, pituitary, parathyroid).

597 Molecular Features of Follicular Variant Papillary Carcinoma of Thyroid: Comparison of Areas with or without Classical Nuclear Features

G Guney, G Guler Tezel, K Kosemehmetoglu, E Yilmaz, R Ersoy, B Cakir, G Guler. Yildirim Beyazit University Ankara Ataturk Research and Education Hospital, Ankara, Turkey; Hacettepe University, Ankara, Turkey.

Background: The purpose of this study was to compare the genetic background of different areas in follicular variant papillary thyroid carcinomas (FVPTC) with or without classical nuclear changes.

Design: Sixteen cases of FVPTC were included to our study. In all 16 cases tumor was well demarcated from surrounding thyroid tissue and they had areas with both full (tumoral areas) and none of the (non-tumoral areas) nuclear changes of papillary carcinoma. DNA is obtained by laser microdissection of both morphological tumoral and non-tumoral areas and point mutations for NRAS codon 61, HRAS codon 61, and BRAF were investigated by direct sequencing. In 11 cases, RT-PCR was performed for the presence of PAX8-PPARγ and RET/PTC1-3 gene rearrangements. Point mutation for NRAS 61 was also studied in 15 colloidal nodules by direct sequencing.

Results: Seven cases (44%) showed at least one mutation; 2 cases (13%) had the same mutation in both tumoral and non-tumoral areas, while in rest only tumoral areas were mutated. None of the studied 11 cases demonstrated RET/PTC1-3 gene rearrangement and in only one case PAX8-PPARγ gene rearrangement was found. Six cases (38%), one of which was both in tumoral and non-tumoral areas, established NRAS codon 61 mutation. Neither HRAS codon 61 nor BRAF were mutated in all cases. Fifteen colloidal nodules were also wild type for NRAS codon 61.

Conclusions: Our findings suggest that NRAS codon 61 point mutations and PAX8-PPARγ gene rearrangement are early events in thyroid carcinogenesis and may be established in selected cases quite before the morphological/phenotypical features fully developed. Therefore, analysis of NRAS codon 61 point mutation seems to be useful especially in diagnosis of follicular variant papillary carcinoma and in cytological specimes with diagnosis of atypia of undetermined significance.

598 Emerin Immunohistochemistry: A Useful Ancillary Test for the Identification of Papillary Thyroid Carcinoma

BH Hinrichs, MD Kinsella, D Lawson, C Cohen, MT Siddiqui. Emory University School of Medicine, Atlanta, GA.

Background: Emerin immunohistochemistry (IHC) highlights unique nuclear membrane irregularities and nuclear shapes characteristic of papillary thyroid carcinoma (PTC). The present study investigates the diagnostic usefulness of emerin IHC in the differentiation of PTC from both follicular neoplasms and non-neoplastic thyroid in histological preparations.

Design: Tissue microarrays (TMAs) consisting of samples from PTC (classic and follicular variant) and non-PTC cases were stained with anti-emerin polyclonal antibody and evaluated for the presence of circumferential nuclear membrane irregularities (garlands), nuclei forming crescent shapes, nuclear grooves, nuclear shape (oval, round, or mixed), intra-nuclear pseudoinclusions, and deep, stellate nuclear membrane invaginations. Staining intensity (strong, intermediate, low, and absent) was also assessed.

Results: Of the 182 TMA cases examined, 95 were diagnosed as PTC (57 classic, 38 follicular variant), and 87 as non-PTC (18 follicular carcinoma, 23 Hurthle cell carcinoma, 6 follicular adenoma, 35 multinodular goiter, 5 normal thyroid).

Emerin staining characteristics, PTC vs non-PTC

Nuclear Features	PTC	Non-PTC	
	% Positive (No.)	% Positive (No.)	p-value
Garlands	100% (95)	6% (5)	<0.0001
Crescent Shapes	72% (68)	13% (11)	<0.0001
Nuclear Grooves	97% (92)	8% (7)	0.002
>75% Oval Shapes	64% (61)	5% (4)	0.001
Pseudoinclusions	65% (62)	34% (29)	0.06
Stellate Invaginations	74% (70)	28% (24)	0.46

Emerin garlands, crescent shapes, nuclear grooves, and oval shapes are nuclear features highly sensitive for both classic and follicular variant PTC. Emerin IHC also demonstrates high specificity for PTC: oval shape, specificity 95%; crescent shape, 92%; garlands, 72%; nuclear grooves, 66%. These observations are all statistically significant ($p<0.05$) determined by linear regression.

Conclusions: Emerin IHC yields patterns in PTC nuclei distinct from those seen in other common thyroid neoplasms and benign conditions. Detection of these patterns in the form of unique nuclear membrane irregularities and nuclear shapes by emerin staining is both sensitive and specific for classic and follicular variant PTC. Emerin IHC is a clinically useful ancillary test for the detection of PTC.

599 Incidence of Thyrioid Malignancy in Completion Thyroidectomy – A Single Institution Experience over Ten Years

Z Hu, Z Ibragimova, U Kapur, RM Wafai, S Mehrotra. Loyola University Medical Center, Maywood, IL.

Background: To do or not to do completion thyroidectomy (CT) for well differentiated thyroid cancers has been subject of debate for several years. While the procedure perse has minimal complications in experienced hands; surgery implies lifelong thyroid hormone supplementation for the patient. In addition many of the CT specimens have benign histology.

Design: A retrospective analysis of histologic findings in CT specimens was performed in patients undergoing the above procedure for a prior malignant diagnosis in lobectomy. The incidence and type of cancer in CT spceimens were assessed and conclusions drawn for rationale of the procedure.

Results: Between 1990 and 2011, 127 patients (female: 102; male: 25, age 48.6 ± 16.1 years) underwent CT. 73 of 127 patients with a diagnosis of either papillary thyroid cancer (PTC) or follicular carcinoma (FC) on lobectomy were included for review. 60 patients had PTC and 13 FC (n=11 minimally invasive and n=2 angioinvasive). 32 of 73 patients had a malignant diagnosis in CT. CT for all minimally invasive FC (n=11) showed benign histology. Of the two angioinvasive FC, one showed residual FC while the other had a microPTC in the CT specimen. The incidence was significantly higher (50%) when CT was performed for a prior diagnosis of PTC; however did not show any association with tumor size or number of tumor foci ($p>0.05$). CT performed for a follicular variant of PTC had a statistically significant ($P<0.05$) incidence of benign histology.

The consistency of malignant diagnosis in initial lobectomy with completion thyroidectomy

	Initial lobectomy	Completion thyroidectomy	%Consistency
Minimally invasive follicular carcinoma	11	0	0%
Angioinvasive follicular carcinoma	2	2	100%
Papillary carcinoma	60	30 (19 microPTC)	50%

The correlation of histologic characteristics of papillary carcinoma (initial diagnosis) to the incidence of malignancy in completion thyroidectomy

Initial diagnosis Classification	Sub-classification	Number of patients (n)	CT diagnosis Benign	CT diagnosis Malignant	p value
Size	<1.0cm (pT1a)	46	26	20	
	1-2cm (pT1b)	11	8	3	>0.05
	>2cm (pT2)	3	1	2	
Focus/foci	1	37	27	10	
	>=2	23	8	15	>0.05
Variants	Conventional	34	15	19	
	Follicular	26	20	6	0.04*

Conclusions: CT with subsequent lifelong thyroid supplementation can be deferred in patients with minimally invasive FC and follicular variant of PTC. We also conclude that due to a high incidence of malignancy in CT for microPTC and no universally accepted protocol for their management, CT is a feasible option in these patients.

600 Characterization of microRNA Expression in Medullary Thyroid Carcinoma

J Hudson, E Duncavage, S Wells, A Tamburrino, P Salerno, L Xi, M Raffeld, J Moley, R Chernock. Washington University School of Medicine, St Louis, MO; National Cancer Institute, Bethesda, MD.

Background: MicroRNAs (miRNAs) are a primordial mechanism of gene expression control that appear to be crucial to cellular development. Recent evidence suggests that differential expression of miRNAs may play an important role in tumor development. Further, expression of certain miRNAs has been associated with tumor prognosis and may be good targets for future therapies. Approximately 25% of medullary thyroid carcinomas (MTCs) are hereditary and harbor germline activating mutations in the *RET* gene. Somatic *RET* mutations are also seen in roughly 50% of sporadic MTCs. We sought to determine the role of miRNA expression in MTC.

Design: DNA and RNA were extracted from formalin-fixed paraffin-embedded tissue blocks of 15 MTCs [10 with *RET* mutations (5 with M918T mutation) and 5 without *RET* mutations] and 5 non-tumor thyroids. Three of the *RET* mutated tumors were from patients with hereditary MTC (all multiple endocrine neoplasia type 2A). Targeted analysis of *RET* mutations in exons 10, 11, and 13-16 was performed by pyrosequencing. MiRNA expression was then quantitated by Real Time PCR using the ABI OpenArray miRNA assay that included over 800 miRNAs. The resulting data were normalized to averaged RNU48 expression for each case.

Results: Compared to normal thyroid, expression of miR-497 (p=0.007), miR-345 (p=0.012), miR-223 (p=0.013) and miR19b-1 (p=0.036) were significantly lower in MTC (both hereditary and sporadic forms). Within MTCs, expression of miR-193b (p=0.011), miR-125a-3p (p=0.015) and miR-10a (p=0.018) were significantly higher in *RET* negative versus *RET* positive MTC. Among *RET* mutated MTCs, miR-149 (p=0.027) and miR-29c (p=0.034) expression were significantly lower in cases with M918T *RET* mutations. Interestingly many of these miRNAs have been implicated in other malignancies.

Conclusions: Using quantitative real time PCR we identified several miRNAs that showed significant changes in expression when comparing MTC to normal thyroid, *RET*-mutated to non-mutated cases, and *RET* M918T-mutations to other *RET* mutations. These data suggest that the biology of MTC may depend on altered miRNA expression. Further, there appears to be differences in miRNA expression profiles between *RET*-mutated and non-mutated MTC, suggesting that *RET*-mutated MTC may result in alterations to different biologic pathways.

601 The Definition of "Sizable" Blood Vessel as a Histologic Clue of Extrathyroidal Tumor Extension Can Be Clarified by Morphometric Analysis of Intra- and Extrathryroidal Blood Vessels

HM Jeon, B Lim, SW Hong. Yonsei University College of Medicine, Gangnam Severance Hospital, Seoul, Republic of Korea.

Background: Collage of American Pathologist cancer protocol suggests that diagnostic findings for minimal extrathyroidal extension includes the presence of carcinoma extending into perithyroidal tissues, including infiltration of adipose tissue and skeletal muscle, as well as around (and into) sizable vascular structures and nerves. However, there are no definite histological criteria of "sizable" vascular structures. Therefore, we have planned to clarify the definition of sizable vascular structures, one of the helpful histologic clues of minimal extrathyroidal extension (ETE).

Design: We hypothesized that the mean thickness of extrathyroidal arteries is significantly different from that of intrathyroidal arteries. Ten total thyroidectomy specimens with papillary carcinoma or microcarcinoma were selected by the even age and sex distribution. Representative slides of each case were analyzed. The number and the wall thickness of the arteries in intra- and extrathyroidal area were evaluated after Elastic Van Gieson (EVG) staining and using a morphometric program. In addition to the arterial wall thickness measurement, we applied immunohistochemical staining of S-100 protein to confirm the absence of nerve tissue in the thyroid parenchyma.

Results: The average numbers of extrathyroidal and intrathyroidal arteries examined in each case were 16.4 and 13.3, respectively. The mean thickness of extrathyroidal (26.9 um, range; 6.1~137.5 um) and intrathyroidal arteries (15.1 um, range; 4.7~58.4 um) was significantly different (p=0.000). The mean thickness of extrathryoidal and intrathyroidal arteries of male (23.5 um and 14.3 um) and female (29.8 um and 15.8 um) were not different (p=0.342 and p=0.084). In addition as we expected, we confirmed the absence of nerve tissue in the thyroid parenchyma by immunohistochemical staining of S100 protein.

Conclusions: This study showed that there is a significant difference in the thickness of extra- and intrathyroidal arterial wall. At least we can suggest that an extrathyroidal artery can be regarded as a "sizable" blood vessel when its thickness is more than 58.4 um.

602 The Increase in Papillary Thyroid Cancer Incidence in the U.S. during the Last Four Decades Is Accompanied by a High and Stable Frequency of *BRAF* Mutations and a Sharp Increase in *NRAS* Mutations

CK Jung, JH Lubin, AV Brenner, MP Little, AJ Sigurdson, YE Nikiforov. University of Pittsburgh, Pittsburgh; The Catholic University of Korea, Seoul, Republic of Korea; National Institute of Health, Bethesda.

Background: The incidence of thyroid cancer in the U.S. has been steadily increasing over the last 40 years, primarily due to the tripling of papillary thyroid carcinoma (PTC) based on Surveillance, Epidemiology, and End Results (SEER) data. However, changes in histopathology and molecular genetics of PTC over this time have not been well studied.

Design: We examined demographic, pathologic and molecular changes in PTC over the past 35 years in 469 cases from one institution. Consecutive PTC cases were studied during four pre-selected periods: 1974-85 (n=127), 1990-92 (n=59), 2000 (n=53), and 2009 (n=230). Histological glass slides were reviewed, and molecular analyses for *BRAF* mutation and three *RAS* mutations (*KRAS, NRAS, HRAS*) were performed on 361 tumors of ≥3 mm in size.

Results: Mean age at diagnosis of PTC cases increased over time from 38 to 51.5 years ($p_{trend}<10^{-12}$), agreeing with SEER data. The proportion of microcarcinomas (≤ 1cm) increased from 33% to 51% ($p_{trend}=0.001$). The prevalence of extrathyroidal extension and lymph node metastasis decreased from 40% to 21% ($p_{trend}=0.0002$) and from 27% to 18% ($p_{trend}=0.04$), respectively. The proportion of all tumors with classic papillary growth pattern decreased (76% to 36%; $p_{trend}<10^{-12}$), whereas tumors with a follicular pattern increased (18% to 57%; $p_{trend}<10^{-12}$). Surprisingly, the prevalence of *BRAF* mutation was stable: 43% in 1974-85 and 41% in 2009. The prevalence of *BRAF* mutation increased in classic papillary variant (53% to 76%; $p_{trend}=0.04$), and showed a trend for increase in the follicular variant (0% to 10%; $p_{trend}=0.09$). The proportion of *RAS* mutations increased from 7% to 25% ($p_{trend}=0.00001$), exclusively due to *NRAS* mutations that occurred in tumors with the follicular variant histology.

Conclusions: Our results suggest that the increase in incidence of PTC over the last four decades was characterized by increased age at diagnosis and detection of smaller-sized, intrathyroidal PTC, and tumors with the follicular growth pattern. However, the increase coincided with a stably high frequency of *BRAF* mutation, arguing against the notion that it is due to detection of clinically irrelevant, non-progressing tumors.

603 An Analysis of Protein Expressions of Pancreatic Neuroendocrine Tumors of Japanease Patients According to 2010 WHO Classification

A Kasajima, K Ishida, F Fujishima, F Motoi, H Ootsuka, Y Nakamura, M Watanabe, M Unno, H Sasano. Tohoku University Hospital, Sendai, Japan.

Background: Results of recent epidermiological studies of neuroendocrine tumor (NET) in Japan demonstrated marked differences in the incidence and locations of the patients between Japan and Western countries. Previous studies have demonstrated the biological interactions among mammalian target of rapamycin (mTOR) signaling pathways, growth factor receptors, such as epidermal growth factor receptor (EGFR), angiogenesis, and anti-angiogenetic actions mediated by somatostatin receptors (SSTRs) in NET. However the status of these factors in Japanese PNET patients has not been studied in details. We therefore evaluated the status of tumor growth regulators, such as mTOR or EGFR, and anti-proliferative regulators, such as SSTRs in order to understand their clinical and/or biological significance in Japanese PNET patients.

Design: Immunoreactivity of hypoxia induced factor 1a (HIF1a), vascular endothelial growth factor (VEGF), mTOR and EGFR were semiquantitatively assessed in 62 cases of surgically resected Japanese PNET cases. Membranous immunoreactivity of five subtypes of SSTRs (1, 2a, 2b, 3, 5) was regarded as positive. The immunoreactivity was compared to clinicopathological findings as well as the new grading system according to WHO classification, tumor size and metastatic status.

Results: Tumor grading of the cases according to WHO2010 was G1: 46.8%, G2: 48.4% and G3: 4.8%. HIF1a, VEGF, mTOR and EGFR were detected in 50 (70.4%), 53 (74.6%), 48 (67.6%) and 29cases(40.8%), respectively. The status of HIF1a and EGFR in G3 NET was significantly higher than in G1/2 NET patients (p=0.026, p=0.014, respectively). No significant association was detected between WHO2010 Grade and VEGF and mTOR status of the tumor.

Conclusions: A significant positive correlation was detected between tumor grading according to WHO 2010 and the status of HIF1a and EGFR in tumor cells. However, VEGF and mTOR status was not significantly associated with with tumor grading. In addition, the status of SSTRs, which have been demonstrated to play pivotal roles in anti-proliferative activities of tumor cells, was not significantly correlated with tumor grading of the Japanese NET patients in our present study, possibly due to relatively low proliferative status of the cases examined. Results of our present study also suggest that both HIF1a and EGFR play important roles in tumor proliferation in Japanese PNET patients.

604 Use of a 92-Gene Molecular Classifier To Predict the Site of Origin for Primary and Metastatic Tumors with Neuroendocrine Differentiation

SE Kerr, CA Schnabel, PS Sullivan, Y Zhang, V Singh, B Carey, MG Erlander, WE Highsmith, EF Brachtel, SM Dry. Mayo Clinic, Rochester, MN; bioTheranostics, Inc., San Diego, CA; University of California at Los Angeles, Los Angeles, CA; Massachussetts General Hospital, Boston, MA.

Background: A diagnosis of neuroendocrine carcinoma (NEC) is typically straightforward using a combination of morphology and immunohistochemical stains (eg. synaptophysin, chromogranin), however, the tumor site of origin may remain elusive in a metastatic presentation. Neuroendocrine tumor subtyping has important implications for staging and management. This study describes the use of a 92-gene molecular cancer classifier for neuroendocrine tumor subtyping.

Design: Seventy-five (44 metastatic and 31 primary) formalin-fixed, paraffin-embedded tumor samples were selected after a 3-pathologist adjudicated review. Clinicopathologic diagnoses were classified as follows for comparison to the molecular classifier output: Intestinal NEC (n=12), high-grade pulmonary NEC (small cell or large cell, n=11), low-grade pulmonary NEC (pulmonary carcinoid, n=11), Merkel cell carcinoma (n=10), pancreatic NEC (n=10), pheochromocytoma/paraganglioma (n=10), and medullary thyroid carcinoma (n=11). Samples were tested in a blinded fashion using the CancerType ID® 92-gene classifier (bioTheranostics, Inc), which makes tumor type predictions based upon expression measurement of 87 gene targets and 5 reference genes by quantitative PCR. The top classifier prediction was compared to the reference diagnosis.

Results: The classifier correctly predicted the reference subtype diagnosis in 71 of 75 cases (95%). Sensitivity, specificity, positive predictive value (PPV), and negative predictive value (NPV) for predicting individual subtypes are shown in Table 1. Three of the 4 incorrectly predicted cases were correctly predicted to the neuroendocrine carcinoma level, but were assigned an incorrect subtype.

Conclusions: The 92-gene classifier demonstrated excellent accuracy for subtyping tumors with neuroendocrine differentiation. While this study did not adjust for subtype prevalence in practice, these results show promise for use in classifying neuroendocrine tumors of unknown primary site.

Table 1. 92-gene Classifier Subtype Performance

Subtype	N	Match	Sens	Spec	PPV	NPV
Intestinal	12	12	1.00	1.00	1.00	1.00
Lung high grade	11	10	0.91	1.00	1.00	0.98
Lung low grade	11	10	0.91	1.00	1.00	0.98
Merkel cell	10	10	1.00	0.97	0.83	1.00
Pancreas	10	8	0.80	0.98	0.91	0.97
Pheo/paraganglioma	10	10	1.00	1.00	1.00	1.00
Thyroid medullary	11	11	1.00	1.00	1.00	1.00
Total	75	71	0.95			

605 Aberrant Expression of the Runx Family Genes in Thyroid Carcinomas

T Kondo, D Niu, T Nakazawa, T Kawasaki, N Oishi, K Mochizuki, T Yamane, R Katoh. University of Yamanashi, Yamanashi, Japan.

Background: The mammalian runt-related transcription factor (Runx) genes, including RUNX1 (AML1/CBFA2), RUNX2 (AML2/CBFA1) and RUNX3 (AML3/CBFA3), encode transcription factors that are master regulators of proliferation and differentiation during embryonic development. Recently, aberrant expression of the Runx family genes and its oncogenic or anti-oncogenic functions have been identified in the progression of human cancers.

Design: In this study, we investigated the expression profile of Runx family genes in normal thyroid tissue, non-neoplastic but abnormal thyroid tissue, various types of thyroid tumors and representative human thyroid carcinoma cell lines.

Results: Using reverse transcriptase polymerase chain reaction and Western blotting, we found that Runx2 was consistently up-regulated in papillary thyroid carcinomas (PTCs) and thyroid carcinoma cell lines compared with normal thyroid tissue. With immunohistochemistry, we observed negative or focal immunoreactivity of Runx2 in the nuclei of normal thyroid follicular cells. None of the non-neoplastic thyroid tissues, including Graves' thyroid and adenomatous goiter, had diffuse positivity of Runx2. Expression of Runx2 in benign follicular adenomas varied from negative to diffusely positive. Meanwhile, all malignant thyroid tumors showed some Runx2 immunopositivity. It was diffuse and intense in 83% (19/23) of PTCs, 71% (5/7) of follicular thyroid carcinomas (FCTs) and 40% (4/10) of undifferentiated thyroid carcinomas (UTCs). In thyroid carcinoma cell lines, the MEK inhibitor U0126 suppressed Runx2 suggesting an association of the MAPK/ERK pathway with Runx2 regulation. Effective silencing of Runx2 by short interfering RNA (siRNA) demonstrated down-regulation of EMT-related molecules (SNAI2, SNAI3 and TWIST1), MMP2 and vasculogenic factors (VEGFA and VEGFC) in thyroid carcinoma cells. We also confirmed that Runx2 silencing suppresses thyroid carcinoma cell invasion in transwell assays.

Conclusions: The present study provides insight into the potential molecular mechanism of thyroid cancer invasion. Our data suggest that enhanced Runx2 is functionally linked to tumor invasion and metastasis of thyroid carcinoma by regulating EMT-related molecules, matrix metalloproteinases and angiogenic/lymphangiogenic factors.

606 Somatostatin Receptor Subtype 2A Immunohistochemistry Using a New Monoclonal Antibody Selects Tumors Suitable for In Vivo Somatostatin Receptor Targeting

M Korner, B Waser, A Schonbrunn, A Perren, JC Reubi. Institute of Pathology of the University of Berne, Berne, Switzerland; Health Science Center Houston, University of Texas, Houston, TX.

Background: High over-expression of somatostatin receptors in neuroendocrine tumors allows imaging and radiotherapy with radiolabelled somatostatin analogues. To know if a tumor is suitable for such an in vivo somatostatin receptor targeting, its somatostatin receptor expression has to be determined. There are specific indications to use immunohistochemistry for the somatostatin receptor subtype 2A (sst2A) for this purpose, but this has up to now been limited by the lack of an adequate reliable antibody. The aim of the present study was to correlate results of immunohistochemistry using the new monoclonal anti-sst2A antibody UMB-1 with those obtained by the gold standard in vitro method ^{125}I-[Tyr^3]-octreotide autoradiography that quantifies somatostatin receptor levels in tumor tissues.

Design: Eighty-nine tumors were subjected to UMB-1 immunohistochemistry and in vitro ^{125}I-[Tyr^3]-octreotide autoradiography. UMB-1 staining levels were semi-quantitatively assessed with respect to the fraction of stained tumor cells and the staining intensity. These UMB-1 staining levels were compared with somatostatin receptor binding site levels quantified with autoradiography.

Results: An immunohistochemical staining threshold was defined to distinguish tumors with somatostatin receptor levels high enough for clinical applications from those with low receptor expression. The presence of more than 10% of tumor cells positive for UMB-1 correctly predicted high autoradiographic somatostatin receptor levels in 95% of cases. Conversely, no UMB-1 staining at all truly reflected low or no autoradiographic somatostatin receptor expression in 96% of tumors. If 1-10% of tumor cells were stained, a weak staining intensity was suggestive of low somatostatin receptor levels.

Conclusions: For the first time, a reliable recommendation concerning the eligibility of an individual patient for in vivo somatostatin receptor targeting can be made based on sst2A immunohistochemistry. Under optimal methodological conditions, UMB-1 immunohistochemistry may be equivalent to in vitro receptor autoradiography.

607 Cellular Localization of Beta-Catenin by Immunohistochemistry Is a Sensitive and Specific Surrogate for *CTNNB1* Mutational Status in Adrenal Cortical Neoplasms

AE Kovach, Q Lam, D Dias-Santagata, PM Sadow. Massachusetts General Hospital, Boston, MA; Harvard Medical School, Boston, MA.

Background: Evaluating adrenal cortical carcinoma (ACC) is a challenge in surgical pathology because of its relative rarity and histologic overlap with adenomas (ACA). We previously performed a molecular screen of adrenal cortical carcinomas and confirmed enrichment of *CTNNB1* mutations in these tumors. Here, we compare mutational status of carcinomas with a cohort of adenomas with comparatively benign clinical outcome and to investigate the relationship between mutational status and beta-catenin (BCAT) nuclear localization by immunohistochemistry.

Design: Twenty-one cases of ACC and 11 cases of ACA underwent histologic and clinical review as well as a multiplex nucleotide amplification molecular screen (SNaPshot) from formalin-fixed paraffin-embedded tissue developed in-house of 15 common cancer-associated genes, including common sites for mutation in the beta-catenin (*CTNNB1)* gene. Immunohistochemistry for BCAT was performed, and sensitivity and specificity for immunohistochemistry to predict mutational status were determined.

Results: By mutational screen, 9/21 carcinomas (43%) had *CTNNB1* mutations, 1 with an additional *p53* mutation; 1 case with an *APC* mutation; and the remaining 11 were wild-type for tested loci. Strong nuclear localization of BCAT immunostain corresponded with the presence of *CTNNB1* mutation by genotyping in 8 of 9 cases (89% sensitivity); the mismatched case demonstrated strong membranous staining by IHC. Nine of the 12 cases without *CTNNB1* mutation by mutational screen showed membranous staining or did not stain (75% specificity). 3 mismatched cases demonstrated scattered (<10%) positive nuclei; 1 of these cases had the APC mutation. 2 of 11 adenomas (18%) demonstrated *CTNNB1* mutations by mutational screen, with no mutations identified in the 9 additional cases; this was corroborated immunohistochemistry for BCAT. No histomorphologic parameter appeared dominant in lesions with a particular mutational status.

Conclusions: Mutational status of *CTNNB1* in adrenal cortical neoplasms can be predicted with reasonable accuracy by immunohistochemical cellular localization. Larger studies are needed to address whether *CTNNB1* mutational status is associated with prognosis of adrenal cortical lesions. Nuclear localization of beta-catenin by immunostain may be helpful in analysis of select lesions of the adrenal cortex whose biologic behavior is uncertain from clinical and histologic information.

608 Cribriform Morular Variant of Papillary Thyroid Carcinoma: Morphological Characteristics of an Unusual Tumor That Distinguish the Inherited and Sporadic Subtypes

CM Kovacs, V Nose. University of Miami, Miami, FL; Jackson Memorial Hospital, Miami, FL.

Background: The cribriform morular variant of papillary thyroid carcinoma (CMv-PTC) is an extremely rare tumor classically known to be associated with familial adenomatous polyposis (FAP). The literature suggests that there is a rare, sporadic form as well. CMv-PTC occurs almost exclusively in females, is well differentiated and has a characteristic appearance on H&E. We reviewed the pathologic findings and associated clinical, laboratory and molecular findings of all cases from our files.

Design: We reviewed the pathologic and immunohistochemical findings of nine cases of CMv-PTC. Clinical histories were reviewed for the presence or family history of FAP, in addition to molecular results. We compared the pathologic findings between the FAP-associated tumors (7/9) and those classified as sporadic (2/9).
Results: All patients were female and ranged from 18 to 53 years of age. The FAP associated tumors were small (0.1 – 1.5 cm), multifocal (range 6 -13 nodules), bilateral and two cases showed lymph node metastases. Histologically, these tumors showed features of CMv-PTC with areas of cribriform, solid and morular growth and abundant fibrosis. The sporadic tumors were unifocal and larger (both 3.0 cm). One case was encapsulated and the other showed a metastatic focus in one lymph node. Histologically, these tumors also had areas of cribriform, solid and morular architecture, though these tumors had significantly less fibrosis than the FAP-associated tumors. The immunohistochemical profile was similar between the two groups, with both groups showing aberrant nuclear and cytoplasmic staining with beta-catenin. The tumors were also positive for galectin-3, CK19, p53 and cyclin D1. HBME1 was negative in the sporadic cases and weak or negative in the FAP-associated tumors. Both subtypes were associated with good prognosis and lacked local invasion.
Conclusions: CMv-PTC occurs sporadically and as an extraintestinal manifestation of FAP. Both groups show similar immunophenotype and architecture with cribriform, morular and solid areas; however, sporadic tumors are unifocal, larger and associated with less fibrosis histologically. It may be possible to differentiate sporadic cases of CMv-PTC from those that are FAP-associated based on size, focality, and amount of fibrosis.

609 Colorectal Poorly Differentiated Neuroendocrine Carcinomas (NECs) and Mixed Adenoneuroendocrine Carcinomas (MANECs): Insights into the Diagnostic Immunophenotype and Search for Prognostic Markers

S La Rosa, A Marando, C Capella. Ospedale di Circolo, Varese, Italy; University of Insubria, Varese, Italy.
Background: Colorectal NECs and MANECs are well recognized entities generally known for their biological aggressiveness and poor patient survival. However, a few published papers have highlighted the existence of a subgroup of tumors with a better survival than expected but, to date, there are no established parameters which usefully identify this category.
Design: In order to better characterize such neoplasms and to identify prognostic indicators, 27 NECs and 12 MANECs were investigated for the following parameters: presence of necrosis, cytologic subtype (small, large, intermediate cell types), lymphovascular invasion, perineural invasion, infiltrative or expanding type of growth, size, level of colonic wall invasion, peritumoral lymphoid infiltration, staging according to UICC and ENETS, expression of transcription factors (TTF1, ASH1, CDX2, PAX5), stem cell markers (CD117 and CD34), and cytokeratin 7 and 20.
Results: Neoplasms were more frequently localized in the right colon and were diagnosed at stage III or IV, independently of the scheme used (UICC or ENETS). The mean follow up time was 36 months. 26/39 (67%) patients died of disease and, in particular, 70% of patients with NECs and 58% with MANECs. 7 patients were alive free of disease after a mean follow-up time of 104 months and other 2 patients died for unrelated causes after a mean follow up time of 190 months. No significant different patient survival was observed between NECs and MANECs. Neoplasms showed a heterogeneous spectrum of morphological and immunohistochemical features, but only large cell subtype, significant peritumoral lymphoid reaction, CD117 immunoreactivity and vascular invasion were significantly correlated with prognosis at univariable analysis. Furthermore, only vascular invasion was an independent prognostic marker at multivariable analysis. In addition to these prognostic features, neoplasms showed different expression of transcription factors, stem cell markers and cytokeratins.
Conclusions: Colorectal NECs and MANECs are a heterogeneous group of tumors showing different morphological features and immunophenotype that should be considered for discriminating among possible differential diagnoses. Among different parameters, the evaluation of vascular invasion seems useful to identify different prognostic categories.

610 Primary Benign Parathyroid Proliferative Lesions: Growth Factor Pathways and Stromal Interaction Responsible of the Growth Patterns

R Lam, A Blanes, SJ Diaz-Cano. King's College Hospital, London, United Kingdom; University of Malaga School of Medicine, Malaga, Spain.
Background: The distinction of primary benign parathyroid proliferative lesions is a challenge with a difficult pathological answer, for which the contributions of cell growth-proliferation, TGFβ and calcium-protein kinase C pathways in this biological process remain unknown.
Design: We selected primary benign parathyroid proliferative lesions with irregularly hyperplastic parenchyma (PTNH, 27) and atrophic peritumoral parenchyma surrounding single (adenomas, PTA, 64) or multiple (MPTA, 16) autonomous lesions (WHO criteria) to analyze cell growth-proliferation (MKI67, AKT1, TERT, CAV2, EGFR, ERBB3, FGFR2, FGFBP1, FOXC2, IGFBP4, MST1R, PDGFRB,TIMP1), TGFβ (TGFB1, TGFB2, TGFB3, SMAD1, SMAD2, SMAD3, SMAD4, CDKN1A, CDKN1B, CDKN2A, CDKN2B) and calcium-protein kinase C (CSF2, FOS, IL2, JUN, MYC, ODC1, PRKCA, PRKCE, TFRC) pathways in a low-density selective cDNA array. Total RNA was extracted, cleaned from normal and neoplastic tissues (RNeasy columns), first-strand cDNA synthesized using T7-(dT24)-oligomer and used as template for cRNA synthesis. The cRNA was fragmented, Cy3-/Cy5-labeled, and hybridized to arrays noncompetitively, cross-validating the results (expression factor>2, significance<0.01). Variables were studied regarding histological diagnosis. Significant variables were then tested on tissue sections by in-situ techniques.
Results: PTA and MPTA revealed significant upregulation (expression factor>2, significance<0.01) of TGFB1, SMAD2, and SMAD4 when compared with PTNH, whereas MPTA differentially overexpressed FN1 and FOS. PTNH showed significant overexpression of CDKN1B, FOXC2, IGFBP4, MST1R, and underexpression of FGFR2 when compared with PTA and MPTA. Remaining genes showed no significant differences.
Conclusions: PTNH growth depends on the balanced interaction with stroma and the insulin-like growth factor pathway (IGFBP4, FGFR2 and MST1R), whereas the autonomous proliferation of adenomas is driven by TGFB pathway. The presence of multiple adenomas is related with abnormal cell adhesion and migration processes (FN1).

611 Identification of New Target Proteins in Parathyroid Carcinomas

O Mete, B Erovic, J Irish, SL Asa. University Health Network, Toronto, ON, Canada.
Background: Adjuvant therapies such as radiotherapy and chemotherapy are not particularly beneficial in the management of parathyroid carcinoma. This creates a challenge when dealing with unresectable recurrent and metastatic disease. Therefore, there is need for effective systemic adjuvant therapy in the management of recurrent or metastatic parathyroid carcinoma. We examined the expression profile of markers that are potential targets for novel therapies in this disease.
Design: We constructed a tissue microarray of parathyroid carcinomas from 10 patients and stained the slides for 32 proteins involved in angiogenesis (PDGFR-α, PDGFR-β, VEGFR2), inflammation (COX-1, COX-2), cell adhesion (MMP-1, CD9, keratin 7), cell cycle (Cdc2p34, cyclin D1, Rb, p27, p21, parafibromin, Bmi-1, 14-3-3σ) and apoptosis (Bcl-2a, Mcl-1, Bcl-Xl, p53) with along some markers of the sonic hedgehog (Smo, Shh, Gli-1, Gli-2, Gli-3, Patch), AKT/mTOR (FOXO-1, AKT, mTOR) and WNT (Wisp-1, Wisp-2, β-catenin) signal transduction pathways. Protein expression was determined using computerized image analysis software (Spectrum Plus©, Aperio).
Results: COX-1, CD9, MMP-1, FOXO-1, VEGFR2, PDGFR-α, PDGFR-β, Gli-1, Gli-2, Gli-3 and patched are diffusely expressed in parathyroid carcinoma. Parafibromin was lost in 90% of cases, along with loss of Rb and p27 in the same tumors.
Conclusions: We have demonstrated for the first time that sonic hedgehog pathway proteins as well as COX-1 are diffusely expressed in parathyroid carcinoma. In addition, markers related to angiogenesis and cell proliferation are also significantly expressed. Our preliminary data suggest that these markers may be targets for novel adjuvant therapies in the treatment of parathyroid carcinoma.

612 Folate Receptor Expression in Human Parathyroids: A Novel Finding with Imaging and Therapeutic Implications

S Muller, RK Halkar, FK Villinger, K Im, SA Safley, J Sharma, CJ Weber. Emory University, Atlanta, GA.
Background: Parathyroid (PT) proliferative diseases have increased 300% in the past 2 decades, affecting more than 30,000 new patients annually in the USA. Preoperative localization of PT is suboptimal in as many as 30% of cases detected by ^{99m}Tc-MIBI, resulting in recurrent or persistent disease. ^{99m}Tc-MIBI concentrates in both thyroid and PT tissue, tissues which are frequently in close association. There is a need for a tracer/imaging tool that concentrates in PT more than in the thyroid. In addition PT carcinoma (CA), albeit rare, has no effective medical treatment.
The folate receptor (FR) is highly expressed on a variety of human cancers and holds promise as a therapeutic and imaging target. The aim of this study is to determine whether normal human PT and PT tumors express FR.
Design: 57 PTs were evaluated for FR expression by IHC: (21 adenomas, 9 1^0 hyperplasias, 13 2^0 hyperplasias, 5 CA, and 9 normal PTs; IRB approval #26334). Normal adjacent thyroid, thyroid nodules (4) and thyroid medullary CA (2) were also evaluated for FR. FR expression in tissue specimens was analyzed using a goat anti-human FR polyclonal antibody (sc-16387, 1:100 dilution; Santa Cruz Biotechnology, Santa Cruz, CA). Known head and neck squamous cell carcinomas positive for FR were used as the positive control. FR expression was considered positive when either cytoplasmic or membranous staining was present.
FR expression in normal PT (1), PT adenomas (6), PT hyperplasias (5), PT CA (1), and normal thyroid (1) was determined by Western blotting according to standard techniques using a polyclonal goat anti-human FR polyclonal antibody.
Results: Normal PT and all PT proliferative disorders showed strong immunoreactivity for cytoplasmic FR. None of the thyroid tissues were positive for FR with the exception of 1 thyroid medullary CA (<10% FR expression).
By Western blotting, a 50 kDa band (FR) was detected in all PT tissue with the exception of 1 PT adenoma and 1 PT CA. No FR expression was detected in thyroid tissue.
Conclusions: This is the first report of FR expression on human PT cells. These findings may hold potential for future investigations including the use of ^{99m}Tc-folate for identification and localization of PT tumors pre-operatively. Additionally, FR expression in PT neoplasms may have therapeutic applications as folate conjugation to anti-cancer drugs may have the potential to be used to deliver therapeutic agents selectively to PT CA.

613 Histopathologic Characteristics of Thyroid Tumors Positive for *BRAF* V600E Mutation

W Nugent, C Coyne, MN Nikiforova, YE Nikiforov. University of Pittsburgh, Pittsburgh.
Background: While large body of information has been accumulated on *BRAF* V600E mutation in papillary thyroid carcinoma (PTC) and its association with histopathological tumor features and a more aggressive behavior, another mutation of this gene, *BRAF* K601E, has not been well characterized. Herein, we report the largest to date series of *BRAF* K601E mutation found in thyroid nodules.

Design: Histopathologic, cytologic and molecular reports for the last five years (06/2007-06/2011) were reviewed to identify thyroid cases with various types of *BRAF* mutation. All case positive for *BRAF* K601E mutation were reviewed to confirm histopathologic diagnosis, tumor variant, and assess other features.
Results: Our analysis identified 548 tumors with *BRAF* mutations identified in the surgically excised of FNA samples. They included 527 (96.1%) V600E mutations, 17 (3.1%) K601E mutations, and 4 (0.8%) other *BRAF* mutation types. Patients with K601E positive nodules were 23-86 year old (average age, 50.3 years), with female:male ration of 3.2:1. Of those, 15 cases had surgical pathology results available for review. Fourteen (93%) of tumors positive for this mutations were papillary carcinomas, and 1 (7%) was follicular carcinoma. Excluding one case that had a complex mutation K601E+T599I, most of K601E-positive papillary carcinomas were of the follicular variant and one tumor was solid variant. Encapsulation was present in all but one case, and 5 cases showed areas of capsular or vascular invasion. Thirteen cases (86.7%) were T1 lesions, and 2 (13.3%) were T2 lesions.
Conclusions: We find that *BRAF* K601E mutation comprises approximately 3% of all *BRAF* mutations found in thyroid cancer. This mutation is strongly associated with the follicular-patterned thyroid cancer, particularly with the follicular variant of papillary carcinoma. In addition, we report for the first time the occurrence of *BRAF* K601E mutation in a follicular thyroid carcinoma. *BRAF* K601E does not appear to be as aggressive as the *BRAF* V600E mutation, and the majority of the tumors positive for this mutation were T1 lesions.

614 Immunohistochemical Detection of Somatostatin Receptor 2a (SSTR2a) and mTOR in the Cases of Neuroendocrine Tumors (NETs) for Appropriate Biotherapy; Experience of a Large Series of Referred Cases

RY Osamura, M Matsuda, T Itoh, C Inomoto, H Kajiwara. Center for Diagnostic Pathology International University of Health and Welfare(IUHW), IUHW Mita Hospital, Minato-ku, Tokyo, Japan; Tokai University School of Medicine, Isehara, Japan.
Background: Somatostatin analoq(SA) is effective in 70% of cases of NET when the tumor cells are immunohistochemically positive for SSTR2a(USCAP 2011). Everolimus inhibits mammalian target of rapamycin(mTOR) and is used for cancer therapy. This study is aimed at to elucidate the overall immunohistochemical positive rate for SSTR2a in a large series of annually increasing 202 referred cases of NETs and, in the selected cases of metastatic pancreatic neuroendocrine carcinoma(NEC) in the liver, to further elucidate both SSTR2a and mTOR in order to suggest the feasibility of mono- or combined biotherapy in this difficult clinical condition.
Design: Formaling-fixed paraffin sections of total 202 cases(since 2006) of NETs(38%pancreas, 8%duodenum, 6%stomach,7%rectum, 23% liver metastases, 16% others) were subjected to the immunohistochemical staining for SSTR2a with specific antibody(Gramsch Laboratories,Gemany). In selected 28 cases of metastatic pancreatic NEC in the lver, immunohistochemical detection of mTOR was also performed using antibody against bioactive phosphorylated mTOR(Cell Signaling Technology,USA).
Results: 59% of all cases were positive for SSTR2a(Volante score 2 and 3)(Fig). In selected 28 cases of liver metastases of pancreatic NEC, 19 cases(69%) were positive for SSTR2a. mTOR was positive in the cytoplasm in total nine cases(32%). Three cases showed the positive staining in more than 20% of the tumor cells with moderate to intense cytoplasmic staining. One case with strong mTOR staining was negative for SSTR2a.
Conclusions: Increase in cases for SSTR2a staining suggests its need for the appropriate biotherapy.
1. 59%(all) and 69%(liver metastases) of NETs showed SSTR2a positivity which suggests the therapeutic response to SA and warrents SA as a first choice of biotherapy in SSTR2a positive cases.
2. In the selected cases of metastatic panreastic NEC in the liver, positive mTOR staining in both SSTR2a-positive and SSTR2a-negative cases may suggest the use of Everolimus as combined therapy with SA or monotherapy for metastatic diseases.

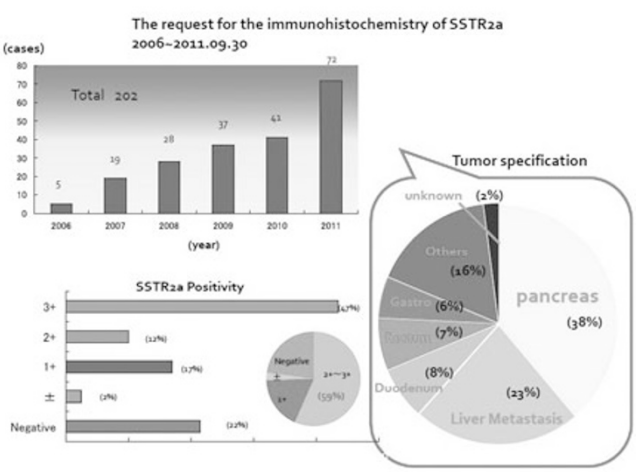

615 Amyloid Deposition in Papillary Thyroid Carcinoma: An Overlooked Event?

A Pinto, V Nose. University of Miami / Jackson Health System, Miami, FL.
Background: Amyloid infiltration in the thyroid is a finding almost restricted to medullary carcinoma. It can also be rarely seen in patients with systemic amyloidosis and amyloid goiter. However, only a handful of cases of papillary thyroid carcinoma (PTC) with amyloid-rich stroma have been reported in the literature.
Design: All cases (paraffin-embedded, hematoxylin & eosin stained slides) of PTC (106 specimens) and benign thyroid (109) from one of our institutions, of a one year period, were reviewed. The cases on which the stroma contained deposits of amorphous, acellular and eosinophilic material characteristic of amyloid**,** congo-red stain was performed and the slides were analyzed under polarized light. The clinical histories of the positive cases were extensively reviewed to exclude patients with primary or secondary systemic amyloidosis.
Results: We found seven (7) patients with amyloid deposition in the thyroid in association with PTC (age ranging from 53 to75 years old), and four (4) cases of benign pathologies (age ranging from 26 to 64 years old; end-stage thyroid- 2 cases, follicular adenoma-1 case, hyperplastic nodule with adenomatous changes- 1 case) diagnosed by the typical apple-green birefringence under polarized light microscopy. Among the positive cases, none of the patients had a known systemic amyloidosis. Most patients were male (7/11), and most of the neoplastic cases had morphological features of a more aggressive behavior (lymphovascular invasion in 5/7; and the variants: diffuse sclerosing-3, tall cell- 1, columnar cell- 1 and oncocytic follicular- 1).
Conclusions: We present the largest series of PTC with amyloid-rich stroma. The relationship between this finding and its real incidence, and if this represents an evidence of a more aggressive behavior when associated with papillary carcinoma, are still unclear statements. However, this study indicates that this finding is not exclusive of medullary carcinoma, since it can be present in other thyroid neoplasms and in benign pathologies. Better characterization of the amyloid will help understand the nature of this phenomenon.

616 The Prognostic Relevance of Nuclear Factor- B Activation in Papillary Thyroid Carcinoma

J-S Pyo, G Kang, D-H Kim, SW Chae, JH Sohn. Kangbuk Samsung Hospital, Sungkyunkwan University School of Medicine, Seoul, Korea.
Background: Although the studies of papillary thyroid carcinoma (PTC) have been focused on the RAS-RAF-MEK-ERK-MAP kinase pathway, the majority of other signaling pathways possibly involved in the tumorigenesis of PTCs have not been fully elucidated. In this study, we investigated the nuclear factor-κB (NF-κB) signaling pathway in PTC using morphoproteomics and correlated the results with clinicopathological parameters.
Design: Immunohistochemistry for NF-κB RelA was performed on archival paraffin-embedded tissues of PTC obtained from 138 patients, and subcellular compartmentalization (nuclear and cytoplasmic) was evaluated.
Results: Nuclear expression of NF-κB RelA regardless of cytoplasmic expression was identified in 94 of 125 PTCs (75.2 %), and was more frequent in PTCs larger than 1 cm ($P < 0.001$). The nuclear expression was not observed in nonneoplastic nodules and benign follicular neoplasms of the thyroid. There were significant differences in the clinicopathological parameters, such as extrathyroidal extension ($P = 0.013$), nodal metastasis ($P = 0.020$), $BRAF^{V600E}$ mutation ($P = 0.033$), cyclin D1 overepxression ($P < 0.001$) and Ki-67 labeling index ($P = 0.042$) between the groups with and without nuclear expression of NF-κB. However, $BRAF^{V600E}$ mutation status and cyclin D1 overexpression was not correlated with any clinicopathological variables.
Conclusions: Our results provide the evidence of activation of NF-κB signaling pathway in PTCs. The expression pattern of NF-κB may serve as a prognostic marker and a potential therapeutic target.

617 Micro-RNA Target Identification, Expression and Immunophenotype Analysis: Possible Role for TRDMT1 in the Pathogenesis of Papillary Thyroid Carcinoma

A Rangel Filho, V Nose. University of Miami, Miami, FL.
Background: Micro-RNA (miR) deregulation has emerged as an important mechanism in human cancers. Multiple studies have shown up-regulation of miR-221, miR-146a, miR-222 and miR-181b in papillary thyroid carcinoma (PTC). We hypothesized that gene targets simultaneously regulated by these four miRs may be involved in pathways important in PTC carcinogenesis. We aimed to identify predicted gene targets of these miRs potentially useful as novel diagnostic or prognostic biomarkers in PTC.
Design: Four miRs, consistently deregulated in PTC were selected. Genome-wide miR target prediction was performed using the mirDB algorithm. Pairwise comparisons of predicted genes identified a common target for all four miRs. In silico validation of the candidate gene was carried out by mining multiple available databases to determine: 1) If RNA and protein gene products are expressed in thyroid; 2) if there is evidence of altered expression in PTC vs. normal thyroid. Target gene product was assayed by IHC in 50 sections of normal and benign/malignant neoplastic thyroid including histological subtypes of PTC.
Results: The gene tRNA aspartic acid methyltransferase 1 (TRDMT1) was the only potential common target of all four miRs. Data mining indicated that: 1)TRDMT1 RNA and protein are expressed in thyroid; 2) Two microarray experiments suggested significant downregulation of TRMDT1 in PTC vs. thyroid ($p < 0.03$ for both). IHC for TRDMT1 was positive in all cases. Combinations of complete nuclear, speckled nuclear, perinuclear, and cytoplasmic staining with variable intensities were observed in both normal and neoplastic cells. Follicular cells showed predominantly positive

nuclear staining. Decreased nuclear and positive cytoplasmic staining was observed in PTCs. This pattern however, was not unique to PTC. Overall, no single combination of staining patterns was able to reliably distinguish among all tumors tested.
Conclusions: We presented an in silico approach to biomarker identification using publicly available experimental data and offered a rationale for prioritization for experimental validation. We identified TRDMT1 as a single common target of 4 miRs reproducibly overexpressed in PTC and documented the patterns of IHC staining in a variety of benign and malignant thyroid samples. In this preliminary study, the limited number of cases analyzed precludes correlation to specific pathologic entities. This limitation will be addressed by continued expansion of the number of cases.

618 Rate of Extrathyroidal Extension and Lymph Node Metastases in Papillary Thyroid Carcinoma with Tall Cell Features

F Rosenblum Donath, S Kraft, JA Barletta. Brigham and Women's Hospital, Boston, MA; Massachusetts General Hospital, Boston, MA.
Background: While papillary thyroid carcinoma (PTC) is generally an indolent tumor, tall cell variant (TCV) is clinically more aggressive than classical PTC. For a tumor to be classified as TCV, at least 50% of the tumor must show tall cell histology. Although it has been recognized that a subset of PTCs have <50% tall cell histology, the significance of this finding has not been established. We designate tumors with <50% tall cell histology as having "tall cell features". In our experience, similar to TCV, these tumors have a high rate of extrathyroidal extension (ETE) and lymph node (LN) metastases; however, these findings have never been formally evaluated. The aim of this study was to investigate the rate of ETE and LN metastases in PTCs with tall cell features and compare these rates to those of classical PTCs.
Design: We studied classical type PTCs and PTCs with tall cell features resected at our institution between 2010 and 2011. Tumors ≤1.0 cm and those with poorly differentiated or anaplastic components were eliminated from the study. For each case the following parameters were recorded: ETE, margin status, vascular invasion, LN status, number of positive LNs, size of the largest LN metastasis, and presence of extranodal extension (ENE).
Results: Our cohort included 99 tumors from 73 women and 26 men, with a mean age at resection of 45 years. Eighty-three (84%) tumors were classical and 16 (16%) had tall cell features. ETE was present in 20 (24%) classical PTCs and 11 (69%) tumors with tall cell features (p=0.0009). Although more tumors with tall cell features had a positive resection margin compared with classical PTCs (25% vs 8%, respectively), this difference did not reach statistical significance (p=0.075). Of cases with sampled LNs (78 cases, 79%), LN metastases were present in 37 (55%) classical PTCs and 10 (91%) tumors with tall cell features (p=0.04). For the tumors with tall cell features with positive LNs, the average number of LN metastases was 9, the mean size of the largest LN metastasis was 2.3 cm (range 0.1-5.5 cm), and the rate of ENE was 30%. In comparison, for the classical PTCs with positive LNs, the average number of LN metastases was 7, the mean size of the largest LN metastasis was 1.1 cm (range <0.1-4.5 cm), and the rate of ENE was 23%.
Conclusions: Our results demonstrate that PTCs with tall cell features have a significantly higher rate of ETE and LN metastases than classical type PTCs, suggesting that these tumors might, like TCV, pursue a more aggressive clinical course.

619 Evaluation of ScreenCell® Devices for the Detection of Circulating Tumor Cells in Adrenocortical Carcinoma

C Scatena, F Salvianti, P Pinzani, M Luconi, M Mannelli, D Massi, G Nesi. University of Florence, Florence, Italy.
Background: Circulating tumor cells (CTCs) are malignant cells found in the bloodstream that originate from the primary tumor or any metastatic localizations. Adrenocortical carcinoma (ACC) is an uncommon and heterogeneous malignancy which gains access to the systemic circulation early during disease progression. To the best of our knowledge, CTC detection rate in ACC patients has not been established. We recently validated a method for CTC detection in melanoma patients, named *Isolation by Size of Epithelial Tumor cells* (ISET), capable of isolating CTCs by filtration of peripheral blood through polycarbonate membranes with 8 µm pores. ScreenCell® filtration devices are novel methods of CTC isolation, based on blood filtration, which enable easy, rapid and open access to CTCs (filtration of 3 ml of peripheral blood is usually completed in approximately 2 minutes), thus avoiding the use of any dedicated instrument.
Design: CTC analysis was performed in 5 ACC patients after peripheral blood was filtered according to the manufacturer's instructions. Weiss score was between 6 and 8, with presence of venous or sinus invasion in all cases. CTC analysis was performed after surgery and in 2 cases the evaluation was also conducted previously. We applied ISET technique in one case and ScreenCell® filtration devices (ScreenCell® CY kit) in the remaining 4 cases.
Results: CTCs were isolated in all 5 (100%) patients. Hematoxylin and eosin stain of isolated CTCs retained cell morphology and were characterized by cell size >16 µm, nucleo-cytoplasmic ratio >50%, irregular nuclear shape and a hyperchromatic nucleus. Cell count number before surgery was consistent with 2.25 CTCs per ml. Similar results were obtained after treatment: 2.025 CTCs per ml were isolated after a median latency from surgery of 13 months. When the analysis was also performed prior to surgery (2 cases), no significant difference in CTC count was observed compared to that carried out after treatment (2 vs. 1.5 CTCs per ml).
Conclusions: We studied the detection of CTCs in ACC patients and demonstrated the suitability of ScreenCell® filtration devices which prove to be an easier method for CTC identification than ISET. Present results build the basis for future larger prospective studies to ascertain whether CTC analysis may be a promising diagnostic tool, providing prognostic information to guide monitoring and treatment in ACC patients.

620 The Changing Panorama of Thyroid FNA; Is Change Good?

VJ Schnadig, MK Kathuria. University of Texas Medical Branch, Galveston, TX.
Background: Use of imaging studies for work-up of non-specific symptoms, cancer staging and other screening has increased. Concomitantly increasing are thyroid "incidentaloma" detection and ultrasound (US) studies. Guidelines have recommended needle aspiration (FNA) of thyroid nodules that are > 1cm. The clinical and demographic data of thyroid FNA performed during the years 1997-98 is compared with those performed during 2009-10.
Design: Computer-search and review of FNA databases were used to find thyroid and total FNA statistics. Chart review was done to determine rate of incidentalomas, mode of aspiration (US vs palpation) and follow-up. Number and percentage of nodules resected and resection diagnoses were compared for the 97-98 and 09-10 periods. Incidentalomas are defined as lesions detected during imaging, such as CT, MRI or US, for problems not related to thyroid.
Results: Total FNA in 97-98 was more than twice that of the 09-10 period, but thyroid FNA increased. In 97-98, 256 thyroid aspirates were done on 232 patients, 9% of 2718 total FNA; 40% of patients were older than 50, and 93% of FNA were done by palpation. Twenty-four patients had repeat FNA but not multiple nodule FNA. During 09-10, there were 281 thyroid FNA on 205 patients, 22% of 1267 total FNA; 60% of patients were older than 50; 96% FNA were US-guided, and 41% of patients had incidentalomas. Radiologist comments encouraging FNA or US evaluation were found in 34% of incidentaloma patients. Multiple nodule aspiration was common. Two nodules were aspirated concomitantly in 60 patients and 3 nodules in 8 patients. Repeat FNA was done in 8 patients. During 97-98, 93 patients (40%) had resections with 26 (28%) adenomas and 20 (21%) cancers (16 DTC, 2 non-thyroid, 1 Hurthle and 1 poorly differentiated). During 09-10, 47 (23%) were resected with 14 (30%) adenomas and 6 (13%) cancers. All cancers were papillary, none were incidentalomas, and 4/6 were younger than 40 years.
Conclusions: There is a trend toward increased US-guided biopsy of incidentally discovered thyroid nodules, often of multiple nodules in an older age group. Resections show predominantly non-invasive neoplasms or other benign conditions, and a very small number of carcinomas are detected. Reported DTC deaths are less than 0.5/100.000. Current guidelines and comments by radiologists may be contributing to an epidemic of US-guided thyroid FNA and follow-up US. We need to acquire unbiased data proving patient benefit.

621 Are Adrenal Lesions Part of the Hereditary Leiomyomatosis and Renal Cell Carcinoma Syndrome (HLRCC)?

B Shuch, M Linehan, MJ Merino. NCI, Bethesda, MD.
Background: Hereditary leiomyomatosis and renal cell carcinoma (HLRCC) is a syndrome characterized by cutaneous leiomyomas, uterine fibroids, and renal cell carcinoma (RCC). Recently, we have observed that HLRCC patients also presented with adrenal nodules, or, adrenal nodules were found at the time of surgery. This study reports our findings to further define if the adrenal lesions are a new component of the HLRCC phenotype.
Design: A prospectively collected database of all HLRCC patients seen at our institution was reviewed for patients with adrenal masses on radiographic imaging. Patient data, imaging studies, endocrine manifestations, management, and pathologic findings were reviewed. Available cases were further studied to look for a loss of heterozygocity (LOH) in the fumarate hydratase gene (FH) by florescence in situ hybridization (FISH) and polymerase chain reaction (PCR).
Results: Twenty of 255 HLRCC patients (7.8%) were identified as having a primary adrenal pathology. Two patients had symptoms of hypercortisolism. Radiographically, three patients had bilateral adrenal lesions (one patient had a solitary nodule in each gland and the other two had two predominant nodules bilaterally). Four patients had multiple bilateral nodules. PET imaging was performed in 10 cases and was positive in 7 (70%). Due to concern for possible malignancy, 9 patients underwent surgery. Pathology demonstrated macro and micronodular adrenal hyperplasia in all specimens. There was no evidence of metastatic disease in any of the glands. PCR and FISH demonstrated that the majority of cases did not demonstrate LOH of FH. The remaining 11 patients are being clinically followed.
Conclusions: We conclude that adrenal micro and macronodular hyperplasia is most likely part of the HLRCC syndrome. A functional endocrine workup as well as adrenal imaging studies should be performed in all patients with suspected or confirmed HLRCC syndrome or germ line FH mutation.

622 Accuracy and Reproducibility of Histologic Features Predictive of *BRAF* V600E Mutation in Papillary Thyroid Carcinoma

RK Virk, A Finkelstein, A Prasad, P Hui, D Chhieng, C Theoharis, J Gibson, S Roman, M Prasad. Yale School of Medicine, New Haven, CT; New York University, New York, NY; Hartford Hospital, Hartford, CT.
Background: We proposed recently that papillary thyroid carcinomas (PTCs) with *BRAF* V600E mutation are morphologically distinct. Here we investigate the accuracy and interobserver reproducibility of a defined set of histological criteria in predicting *BRAF* V600E mutation.
Design: We created a training set of 5 PTCs with and 5 without *BRAF* V600E mutation. The former were classic, tall cell or subcapsular sclerosing variants, and showed well-developed nuclear features of PTC, tall or polygonal cells with moderate to abundant eosinophilic cytoplasm (plump pink cells), stromal fibrosis/sclerosis/desmoplasia, infiltrative tumor borders and psammoma bodies. The latter in general, were follicular variants with subtle nuclear features of PTC, and lacked most or all of the above mentioned histologic features of mutation positive tumors. After self-learning on the training set, two pathologists predicted the presence or absence of *BRAF* V600E mutation

in 30 PTCs (test set) using the morphologic criteria learnt from the training set. The predictions were evaluated against *BRAF* V600E mutational analysis by single strand conformation polymorphism on tumor DNA.

Results: Table 1 shows the sensitivity, specificity, accuracy, and positive and negative predictive values of the histologic criteria for predicting *BRAF* V600E mutation by each pathologists.

Predictive Value of Histologic Features for BRAF V600E Mutation

	Pathologist 1	Pathologist 1
Sensitivity	15/15 (100%)	14/15 (93%)
Specificity	12/15 (80%)	12/15 (80%)
Accuracy	27/30 (90%)	26/30 (87%)
PPV	15/18 (83%)	14/17 (82%)
NPV	12/15 (80%)	12/16 (75%)

There was 'excellent' (kappa 0.795) agreement between the two pathologists for predicting *BRAF* V600E mutation (concordance 27/30; 90%).

Conclusions: Histology can help predict *BRAF* V600E mutation in papillary thyroid carcinomas with accuracy and good interobserver agreement.

623 Papillary Thyroid Microcarcinoma: Clinicopathological Correlation with *BRAF* V600E Mutation

RK Virk, A Finkelstein, A Prasad, P Hui, T Carling, SA Roman, JA Sosa, R Udelsman, M Prasad. Yale School of Medicine, New Haven, CT; New York University, New York, NY; Hartford Hospital, Hartford, CT.

Background: Papillary thyroid microcarcinoma (PTMC: papillary carcinoma ≤1cm) are increasingly being detected due to the frequent use of ultrasonography. Their biology and management remains controversial despite the excellent prognosis. In recent years *BRAF* V600E mutation has emerged as a marker of aggressive behavior in papillary thyroid carcinoma (PTC) but its significance in PTMC is not clear.

Design: Clinical and histopathological features were reviewed in 90 PTMCs. The latter included histologic variant, tumor interface with non-neoplastic thyroid, nuclear features of PTC (well-developed or subtle), presence of cystic change, tall or polygonal eosinophilic (plump pink) cells, extrathyroidal extension (ETE), tumor-associated fibrosis/sclerosis/desmoplasia, stromal calcification, psammoma bodies and osteoclast-like multinucleated giant cells. These features were correlated with *BRAF* V600E mutational analysis performed in all cases by single strand confirmation polymorphism.

Results: Table 1 summarizes significant clinicopathological differences in *BRAF* V600E mutation positive and negative PTMCs.

Clinicopathologic features (n=90)	BRAF V600E mutation positive (n=66;73%)	BRAF V600E mutation negative (n=24; 27%)	p value
Subcapsular sclerosing variant (n=30; 33%)	26 (87%)	4 (13%)	0.04
Follicular variant (n=10; 11%)	3 (30%)	7 (70%)	0.003
Lymph node positive (n=20/65; 31%)	19 (95%)	1 (5%)	0.01
Extrathyroidal extension (n=3; 3.4%)	3 (100%)	0	
Infiltrative interface with adjacent thyroid (n=72; 78%)	60 (83%)	12 (17%)	0.0001
Stromal fibrosis/desmoplasia/ Sclerosis (n=79; 86%)	63 (79%)	16 (21%)	0.0009
Classic well-developed nuclear features of PTC (n=73; 80%)	59 (81%)	14 (19%)	0.001
Multinucleated Giant cells (n=29; 31%)	26 (90%)	3 (10%)	0.02

No significant difference was found between the two groups of PTMCs in age, sex, tumor size, multifocality, psammoma bodies, stromal calcification, cystic change and polygonal eosinophilic tumor cells.

Conclusions: *BRAF* V600E mutation was significantly associated with the subcapsular sclerosing variant of PTMC but not with the follicular variant, and with lymph node metastasis. Histological features characteristic of *BRAF* V600E mutation positive tumors included infiltrative interface with non-neoplastic thyroid, stromal fibrosis/sclerosis/desmoplasia, well-developed characteristic nuclear features of PTC and multinucleated osteoclast-like giant cells.

624 Risk Stratification of Follicular Variant of Papillary Thyroid Carcinoma

M Vivero, S Kraft, JA Barletta. Brigham and Women's Hospital, Boston, MA; Massachusetts General Hospital, Boston, MA.

Background: Recent studies have described an encapsulated and an infiltrative form of follicular variant of papillary thyroid carcinoma (FVPTC). While encapsulated tumors have been reported to have virtually no metastatic potential or recurrence risk, infiltrative tumors have been found to have a significant metastatic potential and a risk of recurrence. In our experience, a substantial number of FVPTCs are neither fully encapsulated nor infiltrative, but instead are partially-encapsulated (PE) or well-circumscribed (WC). The aim of this study was to investigate the metastatic potential and recurrence risk of PE/WC FVPTCs in comparison with that of encapsulated and infiltrative tumors.

Design: We studied 78 FVPTCs resected at our institution between 2000 and 2002. All tumors were evaluated histologically and characterized as encapsulated, PE/WC, or infiltrative. For each case the following parameters were recorded: extrathyroidal extension, margin status, vascular invasion, and lymph node (LN) status. Follow-up clinical information was obtained from electronic medical records.

Results: The tumors in our cohort were from 66 women and 12 men, with a mean age at resection of 50 years. Twenty-seven (35%) tumors were encapsulated, 36 (46%) were PE/WC, and 15 (19%) were infiltrative. LN status was available for 33 (42%) cases, and clinical follow-up was available for 67 (86%) cases. The mean follow-up time was 100 months. LN metastases were absent in all 15 cases of encapsulated tumors and all 9 cases of PE/WC tumors with sampled lymph nodes, but were present in 7 of 9 (78%) cases of infiltrative tumors with sampled LNs. Thus, the LN status was significantly different between PE/WC and infiltrative groups (p=0.0023). No patients with encapsulated tumors recurred, one (3%) patient with a PE/WC tumor recurred, and two (15%) patients with infiltrative tumors recurred. Although the difference in recurrence risk was not significantly different between PE/WC and infiltrative groups (p=0.20), this could be the result of the small cohort size. Interestingly, the one patient with a PE/WC tumor that experienced a recurrence was the only patient in this group that had a positive margin. This patient had a tumor bed recurrence 7 years after initial resection.

Conclusions: Our results demonstrate that PE/WC FVPTCs have a very low metastatic potential/recurrence risk, suggesting that these tumors behave in an indolent fashion similar to that of encapsulated tumors and indicating that they should be distinguished from more aggressive infiltrative tumors.

625 Ribonucleotide Reductase Large Subunit (RRM1) Gene Epression Predicts Efficacy of Adjuvant Mitotane in Adrenocortical Cancer

M Volante, M Terzolo, M Fassnacht, I Rapa, A Germano, S Sbiera, F Daffara, P Sperone, GV Scagliotti, B Allolio, M Papotti, A Berruti. University of Turin, Orbassano, Turin, Italy; University Hospital Wurzburg, Wurzburg, Germany.

Background: Mitotane is the most effective systemic therapy for adrenocortical carcinoma (ACC), but its mechanism of action and possible predictors of treatment response are currently poorly defined. Our aim was to evaluate the gene expression of ribonucleotide reductase large subunit 1 (RRM1) and excision repair cross-complementation group 1 (ERCC1) in ACC as potential biomarkers for clinical outcome, based on their prognostic relevance in other cancer types and on the sequential use of platinum and gemcitabine-based therapy in advanced ACC patients.

Design: Ninety-two tissue samples of completely resected ACC (44 treated with surgery alone, 38 receiving adjuvant mitotane) were centrally analyzed using Real Time PCR for RRM1 and ERCC1 expression. Expression levels were compared to clinical and pathological variables and disease-free (DSF) and overall (OS) survival by means of univariate and multivariate analyses. H295R and SW-13 ACC cell lines were also used for pharmacological tests at different mitotane concentrations. Cell viability was measured using WST-1 assay. RRM1 gene expression was analyzed by means of Real Time PCR. RRM1 silencing experiments were also performed in SW-13 cells.

Results: RRM1 and ERCC1 gene expression levels were reciprocally correlated in the study population (R; 0.4425, p=0.0021) and were not significantly associated with pathological features. ERCC1 gene expression was not significantly associated with DFS and OS neither at univariate nor multivariate analysis. Conversely, high RRM1 expression levels were associated with shorter DFS and OS at both univariate and multivariate analysis. Moreover, in patients with low RRM1 expression, mitotane treatment was associated with a significantly longer DFS than that of patients undergoing follow up only [HR: 0.37; p=0.016], whereas no effect of mitotane treatment on DFS was observed in patients with high RRM1 levels [HR: 1.07; p=0.83], thus suggesting a predictive role of RRM1 gene expression in the mitotane adjuvant setting. In vitro, mitotante-induced RRM1 gene upmodulation was associated to dicreased mitotane sensitivity, and silencing of RRM1 gene in SW-13 cells induced a significant increase in mitotane sensitivity.

Conclusions: Our *in vitro* and *in vivo* data indicate that RRM1 gene expression is functionally associated to mitotane sensitivity and represents the first biomarker in ACC predicting the response to adjuvant mitotane.

626 The Role of MicroRNA Expression in the Diagnosis of Adrenocortical Carcinomas. A Marker of Poor Prognostic Tumors

BA Walter, S Barak, A Fojo, MJ Merino. NCI, NIH, Bethesda.

Background: Adrenocortical carcinoma is an agressive tumor characterized by high metastatic potential and poor patient survival. However, little is known about molecular mechanisms involved in the pathogenesis of these lesions. MicroRNAs (miRNAs), short fragments of non-coding RNAs, have been shown to regulate the expression of genes related with oncogenesis in different tumor types. The aim of this study was therefore to identify miRNAs associated with this malignancy and their potential role in differentiating benign from malignant Adrenocortical lesions.

Design: Fifty one Adrenal lesions were studied: 16 Adrenocortical Carcinomas (AC); 7 metastasis from AC; 8 Adrenal Hyperplasias (AH); 10 Adrenal Adenomas (AA) and their Normal Adrenal (NA) cortex. Tumor and normal subpopulation of cells were microdissected and their RNA extracted. MiRNA expression level of 2 putatively important miRNAs (miRNA 483-5p and miRNA 195) was determined by qRT-PCR analysis of all lesions. Differentially expressed miRNAs for each of the histologic subtypes in comparison with normal adrenal cortex were defined as those with 2-fold change. Immunohistochemical analysis of IGF2 protein expression as a predictor of miR-483-5p target was also evaluated.

Results: In the group of ACs and metastasis, miRNA 483-5p was significantly up-regulated (median fold change 26.98 ($p<0.001$) and 6.15-fold ($p=0.04$), respectively). The higher levels of up-regulation were found in the more aggressive forms of AC. Adrenal Hyperplasia and Adrenal Adenomas showed lower miRNA 483-5p expression levels, (fold change 0.23 ($p=0.13$) and 0.21 ($p=0.12$), respectively). When samples were analyzed as groups (malignant vs. benign) the difference in miR-483-5p expression was highly significant (Fold-change 68.58, $p<0.001$). Inverse results were obtained for miR-195; it was down-regulated in the ACs, and showed very low expression in the metastatic lesions (0.03 ($p<0.001$)). Adenomas and Hyperplasia groups were also down regulated when compared with the normal samples (0.67 and 0.56-fold change). This down regulation was significant when the malignant tumors were compared with the benign group ($p=0.05$).

Conclusions: Our results suggest a relevant role of MiRNA-483-5p and MiRNA-195 in the pathogenesis and diagnosis of Adrenocortical carcinomas. This microRNA signature most likely reflects unique molecular changes for each group of lesions, and it may not only prove to be useful in diagnosis, but it can also have great impact in the development of new molecular targets and therapy.

627 IQGAP1 Copy Number in Follicular-Patterned Lesions of the Thyroid – A Pilot Study

AE Walts, A Riley-Portuges, S Bose. Cedars-Sinai Medical Center, Los Angeles, CA.

Background: The accuracy and reproducibility of the diagnosis of follicular-patterned thyroid lesions (FPTL) is currently limited by subjective morphological criteria and difficulties in assessing capsular integrity and vascular invasion. IQGAP1 is a widely conserved multifunctionl protein currently thought to play an important role in cell polarity, adhesion, migration and proliferation through regulation of the actin microtubule cytoskeleton, transmembrane trafficking, and intracellular signaling. IQGAP1 genetic copy gain has recently been reported in association with increased invasiveness in some thyroid tumors. This pilot study was designed to explore the potential role of IQGAP1 copy number (CN) in the diagnosis of FPTL.

Design: 27 FPTL [10 follicular adenomas (FA), 10 follicular variants of papillary carcinoma (FVPTC), and 7 follicular carcinomas (2 invasive, 3 minimally invasive, and 2 metastases) (FC)] were retrieved from our files. After slides were reviewed and diagnoses confirmed, DNA was extracted from selected areas of two 10-micron sections of each lesion using standard Qiagen QiaAmp FFPE extraction (Valencia CA). Real time PCR detection of gene specific primers (IQGAP1 and a reference gene RNAase) was accomplished using MGB probes (Applied Biosystems). CN was calculated for each sample using the linear region of a standard curve established from a serial dilution and linear regression curve. Histological diagnoses were correlated with CN.

Results: IQGAP1 CN ranged from 1.7 to 3.9. Using a cut-off CN ≥2.5, 2 (20%) of 10 FA, 4 (40%) of 10 FVPTC, and 4 (57%) of 7 FC were positive. Although the percentage of cases with CN ≥2.5 increased from FA to FVPTC to FC, the differences in CN did not reach statistical significance ($p>0.05$) across the three diagnostic groups.

Conclusions: - Increasing percentages of cases with IQGAP1 CN ≥2.5 were observed when FA, FVPTC, and FC were compared.
- IQGAP1 CN may be helpful to stratify FPTL.
- Larger studies are warranted to further assess the potential role of IQGAP1 CN in the diagnosis of thyroid lesions.

628 Validation of BRAF V600E Mutation Using Qiagen Rotor-Gene Analysis System

R Zreik, E Castro-Echeverry, C Chisholm, D Smith, J Gildon, S Walker, K Walker, L Sayage-Rabie, A Rao. Scott & White Memorial Hospital, Temple, TX.

Background: Mutations in the BRAF oncogene are commonly seen in papillary thyroid carcinoma (PTC) and have been shown to be useful in cases of indeterminate cytology from thyroid fine needle aspirations (FNA). Mutation analysis can be performed on a variety of platforms with different diagnostic sensitivities. We present a validation study for BRAF mutational analysis of thyroid FNA samples on the newly introduced Qiagen Rotor-Gene Q platform which uses high resolution melting post-PCR analysis and compare it to results obtained by sequencing and final surgical specimen diagnosis.

Design: Ultrasound guided thyroid FNA samples were obtained. Non-enriched FNA samples were used. DNA was extracted from the specimens using the Roche MagNA Pure Compact extraction kit and was evaluated for the BRAF V600E mutation using the Qiagen PyroMark Q24 sequencer and Qiagen Rotor-Gene Q analysis system. The results were compared to the final surgical diagnosis (gold standard) to determine the sensitivity, specificity, positive predictive value (PPV), and negative predictive value (NPV).

Results: 50 patients were identified for this study and 56 FNA samples were tested (Table 1). In this data set, 6 FNAs were indeterminate and 14 FNAs were diagnostic for PTC. 17 patients were diagnosed with PTC following total/partial thyroidectomy and 9 had metastatic disease. The FNA DNA quantity ranged from 0.34-32.07 ng/µL and the mutation prevalance ranged from 8%-34%.

Table 1: Comparison of Rotor-Gene, PyroMark Q24, and FNA to surgical diagnosis

	Rotor-Gene	PyroMark Q24	FNA
Sensitivity	14/19 (73.7%)	12/19 (63.2%)	17/19 (89.5%)
Specificity	37/37 (100.0%)	37/37 (100.0%)	34/37 (91.9%)
PPV	14/14 (100.0%)	12/12 (100.0%)	17/20 (85.8%)
NPV	37/42 (88.1%)	37/44 (84.1%)	34/36 (94.5%)

Conclusions: When compared to the PyroMark Q24 platform, the Rotor-Gene platform showed superior sensitivity and identical PPV. The Rotor-Gene is capable of successfully analyzing extremely small amounts of DNA and has an improved sensitivity when looking at the identification of metastatic disease. The results in this small cohort suggest that the Rotor-Gene platform BRAF mutation detection could be a useful tool in indeterminate FNA samples.

Gastrointestinal

629 Novel Chromosomal Abnormalities in Barrett's Esophagus and Esophageal Adenocarcinoma Identified by Array Comparative Genomic Hybridization (CGH)

A Agarwal, T Appleberry, S Guha, J Ajani, W Hofstetter, S Swisher, P Lennon, A Rashid, D Maru. The University of Texas M.D.Anderson Cancer Center, Houston; PerkinElmer, Inc, Waltham; Pathgroup, Nashville.

Background: Prior genome wide studies using biopsy samples of Barrett's esophagus (BE) and esophageal adenocarcinoma (EAC) have shown gains of chromosomes 1q, 7q, 8p and losses of chromosomes 3p, 9p, 16q, 17p, and 21q22. Present study performed array CGH on carefully macro dissected fresh frozen tissue samples of BE and EAC and found novel regions of chromosomal alterations.

Design: The study comprised of 14 patients (M:F;11:3, average age 68 years) with BE associated EAC who underwent esophagogastrectomy without preoperative chemoradiation. Tumor stage was T1aN0 in 4, T1bN0 in 6, T1bN1 in 1, T2No in 2 and T4N2 in 1. H&E section of fresh frozen samples from squamous mucosa, non-dysplastic BE and EAC from the resection specimens were reviewed and area with more than 80% of lesion was macrodissected from the frozen block followed by DNA extraction using TRIzol Reagent (Life Technologies, CA) with post-PCR purification. Microarray analysis was performed using bacterial artificial chromosome (BAC) DNA microarrays (Constitutional Chip 4.0, PerkinElmer, Finland). This microarray has over 5200 BAC clones, including targeted coverage in well-characterized chromosomal regions, subtelomeric regions, and pericentromeric regions, as well as backbone coverage of the genome with an average resolution of 0.5 Mb. DNA extracted from either BE or EAC tissue was analyzed using DNA from squamous mucosa from the same patient as a reference. Arrays were scanned at 10 microns using a ScanArray Gx scanner (PerkinElmer) and analyzed using GenePix Pro 6.1 (Molecular Devices, CA).

Results: In BE, gains of chromosomal loci 1p36.33, 1p36.32, 3q21.3, 9q34.2, 9q34.3, 12q24.31, 12q24.33, 16p13.3, 16q24.3, 20q13.3, 21q22.3, 22q13.32 were present in two (18%) samples and losses of loci 9p21.3 in two (18%) samples. The remaining eight BE samples showed no chromosomal gains or losses. All EAC samples showed chromosmal gains. Six (43%) EAC showed gain of chromosomal loci 8p23.1 and 20q13.33, and four (37%) of 7p12.3 and 8q24.3. Other chromosomal gains included 5p15.33, 7p12.3, 7p11.2, 7q11.21, 7q21.13, 7q21.2-21.3, and 8q24.13 in 3 or less tumors. Loss of chromosome Yq11.22 was seen in all EAC from men.

Conclusions: There is marked increase in gains at multiple chromosomes in EAC as compared to BE. Present study supports prior studies showing gains of chromosomal locus 8p23.1 and identifies gain of chromosomal locus 20q13.33 and loss of locus Yq11.22 as novel abnormalities in EAC.

630 Immunohistochemical Features of Intestinal and Foveolar Dysplasia in Barrett's Esophagus

AT Agoston, RD Odze, GY Lauwers, A Srivastava. Brigham & Women's Hospital, Boston, MA; Massachusetts General Hospital, Boston, MA.

Background: Recently, two major subtypes of dysplasia in Barrett's Esophagus (BE) have been identified, termed "intestinal" (INT) or "gastric", also referred to as "foveolar" (FOV). Some patients show a mixture of both types. Previous data have shown that these two subtypes of dysplasia may have different biological characteristics, arise from different types of BE mucosa, and may have different natural history and risk of malignancy. The aim of this study was to determine the immunohistochemical characteristics of these dysplasia subtypes in BE, with emphasis on the type of differentiation (intestinal vs. gastric) present in both.

Design: Thirty-eight BE-related endoscopic mucosal resections (EMR) were evaluated morphologically for the highest grade (low, high) and type of dysplasia (INT, FOV, mixed) by routine H&E histologic methods. Immunohistochemistry was performed for intestinal markers (CDX2, MUC2, and villin) and gastric markers (MUC5AC, MUC6) and for Ki67 and P53, and all markers were scored for the presence and degree of staining in a semiquantitative fashion (grade 0=negative, 1=focal, 2=multifocal, 3=diffuse staining). Staining was compared between the different types of morphologic dysplasia.

Results: By morphology, 11 (29%) were considered intestinal, 8 (21%) foveolar, and 16 (42%) mixed dysplasia. By immunohistochemistry, morphologically classified INT dysplasia showed significantly higher expression of INT markers, such as MUC2, CDX2, and villin, whereas FOV dysplasia showed significantly more MUC5AC and MUC6 expression. Mixed INT/FOV dysplasia showed an immunophenotypic pattern that matched, roughly, the morphologic areas of INT and FOV dysplasia. No significant differences were observed in P53 or Ki67 proliferative index. Interestingly, despite differences in quantity of the various INT and gastric immunomarkers in INT and FOV dysplasia, respectively, all cases of both types of dysplasia showed at least focal CDX2 staining.

Conclusions: Regardless of the morphologic phenotype of dysplasia, whether INT or FOV, all dysplastic epithelium shows some evidence of intestinalization characterized by at least focal CDX2 staining, similar to the background non-dysplastic metaplastic columnar epithelium as previously reported. In general, INT dysplasia shows more advanced INT immunophenotype, in contrast to FOV dysplasia which shows a more advanced gastric phenotype. Further studies are needed to determine whether dysplasia types with more advanced INT versus gastric differentiation have a different risk of malignancy.

631 Goblet Cells Are Depleted with Advancing Degrees of Preneoplasia in Barrett's Esophagus

AT Agoston, A Sanpavat, RD Odze, A Srivastava. Brigham & Women's Hospital, Boston, MA.

Background: A previous study by our group showed that the proportion of goblet cells in index biopsies of patients with Barrett's Esophagus (BE) is inversely proportional to the risk of malignancy, and this led to the hypothesis that goblet cells may represent a successful adaptive form of metaplasia that protects the mucosa from the carcinogenic effects of reflux. However, the topographic distribution of goblet cells in relationship to neoplasia is unknown, and no prior studies have evaluated resection specimens where anatomic distribution can be more accurately noted. The aim of this study was to evaluate the goblet cell density in adjacent non-neoplastic BE both adjacent to, near, and distant from areas of neoplasia in BE patients who had a resection for dysplasia or carcinoma without neoadjuvant therapy.

Design: Routinely processed resection specimens from 40 patients who had a distal esophagogastrectomy for high-grade dysplasia (N=1) or adenocarcinoma (N=39) were evaluated histologically for the mean number of goblet cells per crypt (GC/crypt) in areas adjacent to (<10 crypts), near (10-20 crypts) and distant from (>20 crypts) areas of neoplasia. Goblet cell counts were compared between different mucosal locations in proximity to neoplasia in all cases, and then also compared between areas of low vs. high-grade dysplasia.